

**A Reproduced Copy
OF**

NASA TM-84969

**Reproduced for NASA
by the
NASA Scientific and Technical Information Facility**

REPRODUCED COPY

1984

LANGLEY RESEARCH CENTER
LIBRARY, NASA
HAMPTON, VIRGINIA



Technical Memorandum 84969

RAIN ESTIMATION FROM SATELLITES: AN EXAMINATION OF THE GRIFFITH-WOODLEY TECHNIQUE

A. J. Negri, R. F. Adler and
P. J. Wetzel

(NASA-TM-84969) RAIN ESTIMATION FROM
SATELLITES: AN EXAMINATION OF THE
GRIFFITH-WOODLEY TECHNIQUE (NASA) 43 p
HC A03/MF A01

CSCL 04B

N84-13735

63/47 Unclass
42983

JANUARY 1983

National Aeronautics and
Space Administration

Goddard Space Flight Center
Greenbelt, Maryland 20771

NA

N84-13735 #

TM 84969

RAIN ESTIMATION FROM SATELLITES: AN
EXAMINATION OF THE GRIFFITH-WOODLEY TECHNIQUE

Andrew J. Negri

Robert F. Adler

Peter J. Wetzel

Goddard Laboratory for Atmospheric Sciences (GLAS)

January 1983

GODDARD SPACE FLIGHT CENTER
Greenbelt, Maryland

RAIN ESTIMATES FROM SATELLITES: AN EXAMINATION OF THE GRIFFITH-WOODLEY TECHNIQUE

Andrew J. Negri
Robert F. Adler
Peter J. Wetzel

ABSTRACT

The Griffith-Woodley Technique (GWT) is an approach to estimating precipitation using infrared observations of clouds from geosynchronous satellites. It is examined in three ways: an analysis of the terms in the GWT equations; a case study of infrared imagery portraying convective development over Florida; and the comparison of a simplified equation set and resultant rain map to results using the GWT. The objective is to determine the dominant factors in the calculation of GWT rain estimates.

Analysis of a single day's convection over Florida produced a number of significant insights into various terms in the GWT rainfall equations. Due to the definition of clouds by a threshold isotherm the majority of clouds on this day did not go through an idealized life cycle before losing their identity through merger, splitting, etc. As a result, 85% of the clouds had a defined life of 0.5 or 1 h. For these clouds the terms in the GWT which are dependent on cloud life history become essentially constant. The empirically derived ratio of radar echo area to cloud area is given a singular value (0.02) for 43% of the sample, while the rainrate term is 20.7 mm h^{-1} for 61% of the sample. For 55% of the sampled clouds the temperature weighting term is identically 1.0. Cloud area itself is highly correlated ($r = 0.88$) with GWT-computed rain volume. An important, discriminating parameter in the GWT is the temperature defining the coldest 10% cloud area.

The analysis further shows that the two dominant parameters in rainfall estimation are the existence of cold cloud and the duration of cloud over a point. This leads us to conclude that the GWT is unnecessarily complicated for use in estimating daily rainfall over large areas. Simplifying assumptions are made to the GWT such that the resultant equations are independent of cloud life history, cloud area, and grid square area. Application of a simple algorithm incorporating these assumptions leads to a daily rainfall pattern very similar to that calculated from the GWT for one case study day. We present an in-depth analysis of the storm which caused the only significant difference between the two isohyetal maps.

RAIN ESTIMATION FROM SATELLITES: AN EXAMINATION OF THE GRIFFITH-WOODLEY TECHNIQUE

1. INTRODUCTION

The recent Workshop on Precipitation Measurements from Space (1981) at NASA/Goddard Space Flight Center stressed the need for spaceborne measurements of precipitation across the spectrum of scales from flood warnings to global climate systems. The workshop participants discussed a variety of visible and infrared (IR) methods for observing cloud properties and using them as proxy variables for precipitation. One such method is the Griffith-Woodley Technique (GWT), an approach to estimating precipitation from observations of clouds in the 11 μ window channel from geosynchronous satellites (Griffith *et al.*, 1976). Briefly, the GWT:

- 1) defines and tracks clouds by the outline of the 253K isotherm;
- 2) estimates a cloud rain volume (R_v) through an algorithm that:
 - a) relates the rain area (echo) to the life history of the cloud area;
 - b) relates the rain rate to the life history of the rain area (echo);
 - c) enhances the R_v by a weighting term based on the distribution of cloud-top temperature;
- 3) produces a daily rain map by apportioning the calculated R_v to grid squares by concentrating the rain in the coldest portions of the cloud.

The purpose of this paper is to examine the GWT in three ways: an analysis of the magnitude and variability of the terms in the GWT equations; an examination of infrared (IR) imagery in terms of GWT-defined clouds and their life cycles; and thirdly, the application of a simplified equation set and the resultant comparison to the GWT results. The objective is not to improve the GWT, nor to propose a new technique. Rather, we wish to determine what are the *dominant* factors in the production of GWT rain estimates.

At the core of the original GWT are empirical relationships between the temporal history of satellite-determined visible cloud area and gage/radar measured rainfall over southern Florida (Griffith *et al.*, 1976). These relationships were redefined as functions of cloud-top temperature (CTT) when digital IR data became available. Rainfall estimates were subsequently determined for southern Florida, tropical regions in South America, and for selected Atlantic hurricanes (Griffith *et al.*, 1978). A scheme to apportion the total rain volume of cloud segments were constructed (Woodley *et al.*, 1980) and modified (Augustine *et al.*, 1981) and isohyetal maps of GATE B-scale rainfall were generated. The GWT has also been applied to the U.S. High Plains (Griffith *et al.*, 1981). These results were adjusted in one of two ways: by gage/satellite comparisons for a small area; or by noting differences in the local sounding compared to a mean tropical sounding. This latter adjustment factor was based on output from the Simpson-Wiggert (1969) one-dimensional cumulus cloud model. Recently, Meitin *et al.*, (1981) have used the GWT to construct isohyetal maps for 51 days during the Florida Area Cumulus Experiment (FACE-2).

That rainfall and cloud parameters are highly correlated, especially over large time and space scales, has been shown by several investigators. Arkin (1979), for the GATE B-array (10^5 km^2), showed correlation coefficients as high as 0.88 between 6 h accumulated rainfall and the fraction of the array covered by cloud higher than 10 km (based on an IR threshold CTT). This compares to the coefficient of 0.87 found by Woodley *et al.* (1980) between rain estimated by the time and temperature dependent GWT and verification rain from radar. Garcia (1981) estimated GATE rainfall using the simple Kilonsky-Ramage (1976) regression equation in conjunction with *one* satellite image per day. Cumulative GATE phase estimates (17-20 day period) were highly correlated with GWT estimates, both in rain volume and isohyetal pattern.

This paper will confine itself to the discussion of *daily* rainfall, and will examine the fundamental unit of estimation in the GWT, the half-hourly rain calculation. Following a brief review

of the GWT, data on GWT-derived cloud statistics are presented for one case study day. A discussion of some implications of these data leads us to propose (and quantify) several simplifying assumptions. These are then applied to IR imagery, producing a daily rain map and resultant comparison to the GWT results on that day.

2. A BRIEF SUMMARY OF THE GWT

In brief, the steps necessary to produce a rain depth (D_{ij}) at grid square (ij) at each time interval are:

- 1) From a sequence of IR imagery, identify and compute the area (A_c) of every entity bounded by a 253K isotherm.
- 2) Determine successive values of A_c for each entity until terminated by a split, merger, mingle (simultaneous split and merger) or until lost through evaporation. Entities (clouds) resulting from such interactions are considered new entities.
- 3) Determine the maximum areal extent (A_m) of the entity and use it to normalize each observation of A_c during the lifetime of the entity.
- 4) Use the curves presented in Fig. 1 to determine the fractional area containing precipitation (A_e/A_m), where A_e is the inferred echo (rain) area. Enter the ordinate of Fig. 1 based on:
 - a) The value of A_m (indicates which diagram to use)
 - b) The value of A_c/A_m
 - c) The sign of $\Delta A_c/\Delta t$ where Δt is the interval between satellite images (typically 30 min).

ORIGINAL PAGE IS
OF POOR QUALITY

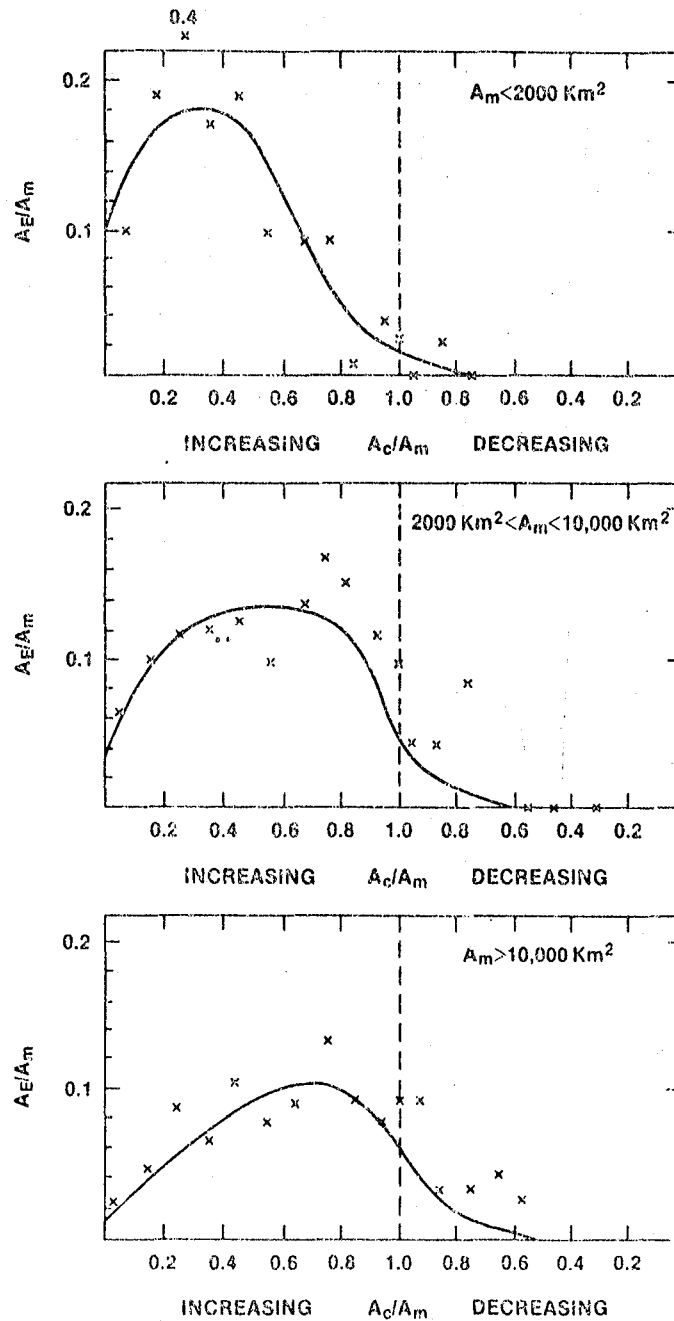


Figure 1. Cloud area/echo area relationships for infrared data in the GWT. Curves are subjective fits to mean data (x's) and are stratified by maximum cloud area. (Adapted from Griffith *et al.*, 1978).

The empirical relationships in Fig. 1 are based on 281 observations of radar echoes and IR defined clouds over southern Florida (Griffith *et al.*, 1978).

- 5) Multiply the fractions A_e/A_m by A_m to determine the life history of A_e . Determine the maximum areal extent of echo ($A_{e(max)}$) and use it to normalize each A_e value.
- 6) From the value of $A_e/A_{e(max)}$ and from the sign of $\Delta A_e/\Delta t$ enter the ordinate of Fig. 2 and determine the rainrate (I). This relationship was derived from digitized WSR-57 radar data from Miami (Woodley *et al.*, 1980, Griffith *et al.*, 1980). The singular point at 20 mm hr⁻¹ in Fig. 2 is for echoes at their maximum area.
- 7) Compute the term $\sum_{i=1}^3 a_i b_i$ for each entity at each time where:

a_1 is the fraction of A_e between 253 and 225K;

a_2 is the fraction of A_e between 224 and 202K;

a_3 is the fraction of A_e less than 201K;

and where b_1, b_2, b_3 are the empirically derived coefficients 1.00, 2.19, and 3.24. This temperature weighting term would be 1.0 (3.24) for a cloud composed entirely of pixels at 253K (201K). It is designed to increase the rain volume for clouds with colder internal temperature structure. These coefficients, empirically derived, were originally based on comparisons between radar echoes and the visible brightness contours in hurricanes (Griffith *et al.*, 1976). The infrared coefficients are described in the appendix of Griffith *et al.*, (1978).

- 8) Compute the rain volume (R_v) for each entity at each time:

$$R_v = I A_e \sum_{i=1}^3 a_i b_i \Delta t \quad (1)$$

ORIGINAL PAGE IS
OF POOR QUALITY

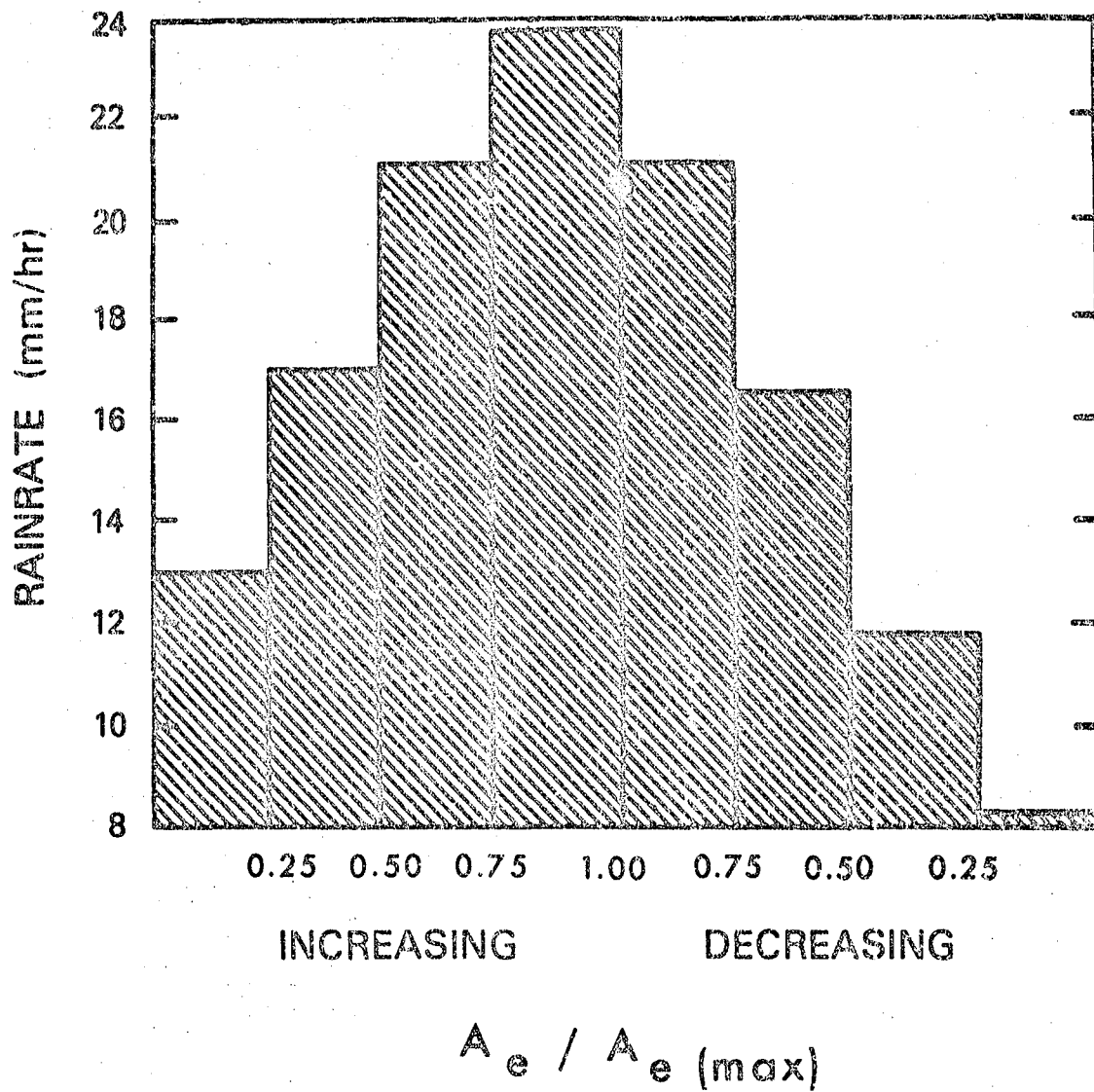


Figure 2. The echo area/rainrate relationship in the GWT, normalized by maximum echo area. The singular point at 20 mm h⁻¹ is for echoes at their maximum area. (Adapted from Griffith *et al.*, 1980).

- 9) Apportion half the rain volume to the coldest 10% of the cloud entity area, and the remaining half to the next warmest 40% of the cloud. For the GATE data, rainfall was apportioned to the whole cloud (Woodley *et al.*, 1980). For estimation in the U.S. High Plains rain was apportioned to the inferred echo area, typically 6% of the cloud area (Griffith *et al.*, 1981). For tropical systems, the "10-50/40-50" apportionment is used (Augustine *et al.*, 1981). Within these 10% and 40% areas the rain is apportioned based on the summation of a parameter b . These summations $[(\Sigma b)_{10\%}$ and $(\Sigma b)_{40\%}]$ run over the cloud pixels in the coldest 10% and next warmest 40% cloud areas respectively.

The b values are given by:

$$b = \exp(1.784095 - 0.03094 T)/11.1249 \quad (2a)$$

when $-31 < T < -20^\circ \text{C}$

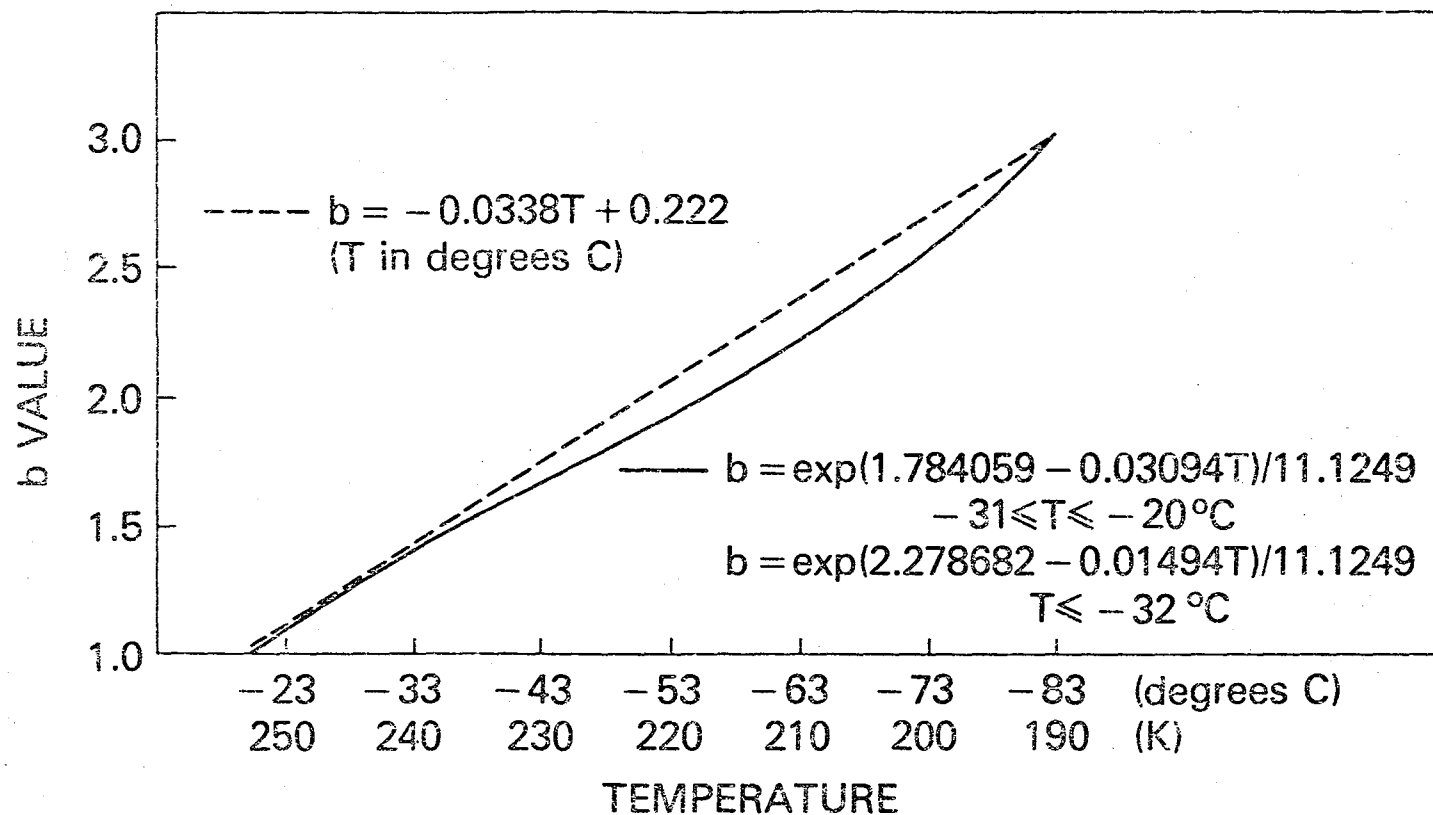
$$b = \exp(2.278682 - 0.01494 T)/11.1249 \quad (2b)$$

when $T < -32^\circ \text{C}$

Equations (2a) and (2b) are plotted as the solid line in Fig. 3 indicating a near linear relationship between b and T (dashed line). These b values are related to the b_1 , b_2 , b_3 of the preceding section. However, there is a small discrepancy when b_2 and b_3 are calculated using Eq. 2b (C. Griffith, personal communication). The b values are expressed in terms of percent of gray scale (P) in Griffith *et al.* (1978) and in terms of digital count (D) in Griffith *et al.* (1980). It is unclear how many data points were actually used to empirically derive these b values.

- 10) Apportion a rain depth (D_{ij}) to grid square area (a_{ij}) on the basis of grid square temperature (T_{ij}):

$$D_{ij} = \frac{R_v b_{ij}}{2a_{ij} \Sigma b_k} \quad (3)$$



ORIGINAL PAGE IS
OF POOR QUALITY

Figure 3. Weighting coefficients as a function of temperature in the GWT (solid curve) adapted from Griffith *et al.*, (1980). The dashed line shows a linear approximation.

where b_{ij} is the result of applying (2a) or (2b) to T_{ij} and where $\Sigma b_k = \{\Sigma b\}_{10\%(40\%)}$ if b_{ij} corresponds to a temperature in the coldest 10% (next 40% warmest) area of the cloud entity.

3. DATA

The case study data set consists of GOES infrared digital imagery on 31 July 1980, one of 51 days during FACE-2 on which the GWT was applied (Meitin *et al.*, 1981). The day was chosen because it was the only day of the 51 on which processed, navigated GOES images previously existed on the Atmospheric and Oceanographic Information Processing System (AOIPS) at the Goddard Space Flight Center. Imagery over the Florida area between 1600 and 0030 (all times are GMT) are displayed in Figs. 4-6. The small, trapezoidal area is the FACE target region. The data have been enhanced to highlight CTT regions which affect the calculation of rain volume in the GWT: black: 252-225K; gray: 224-202K; and white: < 201K. Every black-outlined feature (< 253K) would be defined as a cloud "entity" in the GWT.

The day appears to be representative of convective development over the Florida peninsula, i.e. mostly clear at 1600 with convective clouds growing during the afternoon. By 0030 the anvils of many thunderstorms have merged to form one cloud entity (as defined by the 253K isotherm). This sequence of imagery will be frequently referred to in subsequent sections in which we examine in detail the impact of the various terms in the GWT equations on the final rainfall estimate.

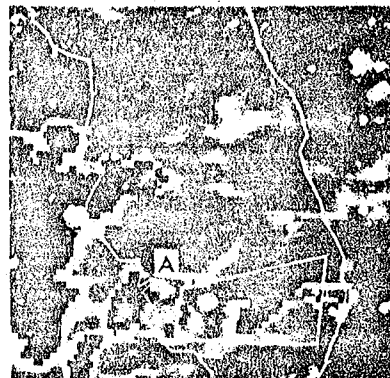
4. CLOUD STATISTICS FOR 31 JULY 1980

It was not possible (nor was it the intent) to replicate the cloud isolation and tracking software utilized by the GWT. Rather, the imagery in Figs. 4-6 are viewed in time sequence. A subjective determination is made as to whether a cloud entity (as defined by the 253K isotherm) either existed on the prior image, is an entity new to that image, or is the result of a split (or merger) of the boundaries of existing entities. We are attempting to simulate the life history relationships

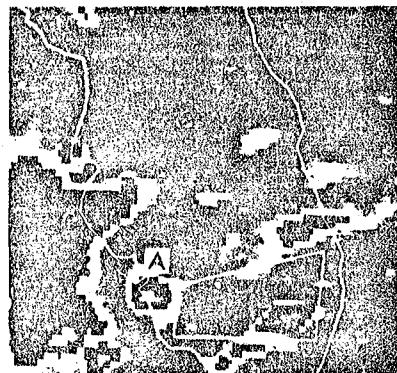
ORIGINAL PAGE IS
OF POOR QUALITY



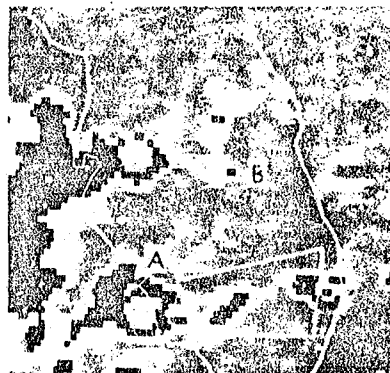
1600 GMT



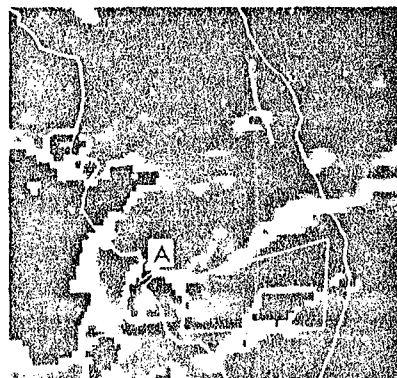
1730 GMT



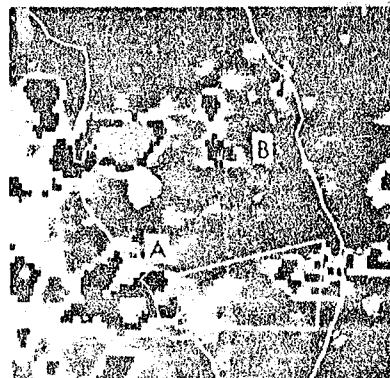
1630 GMT



1800 GMT



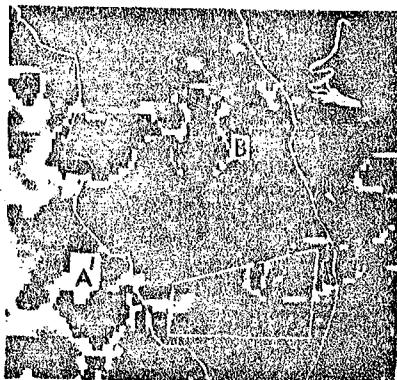
1700 GMT



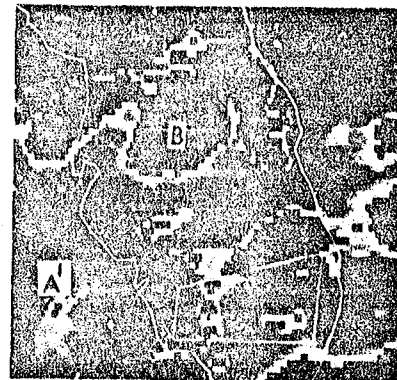
1830 GMT

Figure 4. GOES infrared imagery 1600-1830 GMT 31 July 1980. The area is approx. 500 km on a side and the FACE target area is outlined by the small trapezoid. Enhancement: Black: 253-225K; Gray: 224-202K; and White: < 201K.

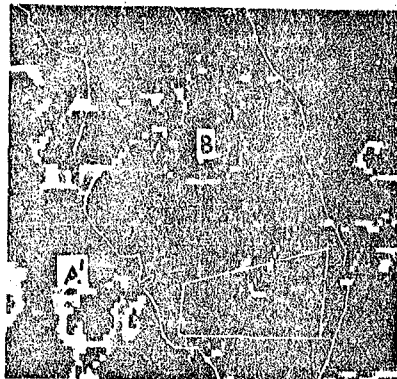
ORIGINAL PAGE IS
OF POOR QUALITY



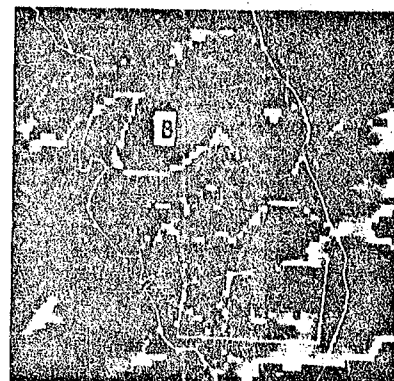
1900 GMT



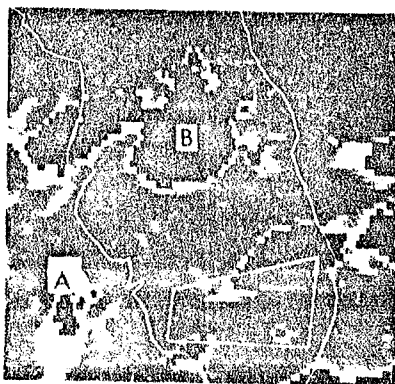
2030 GMT



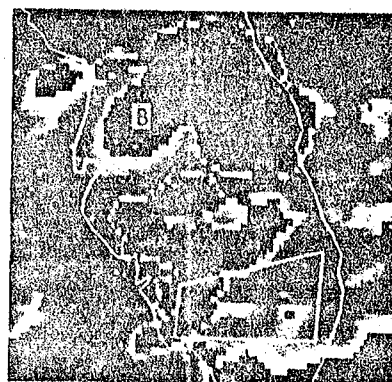
1930 GMT



2100 GMT



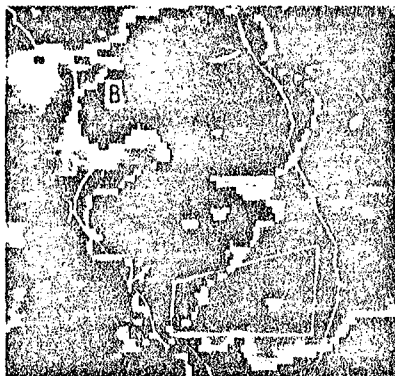
2000 GMT



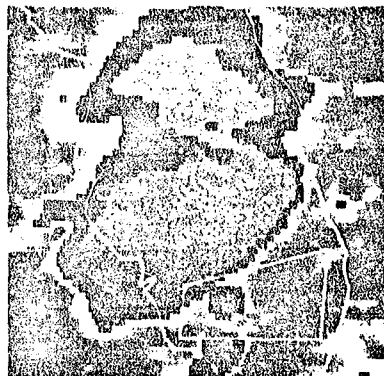
2130 GMT

Figure 5. GOES infrared imagery 1900-2130 GMT 31 July 1980.

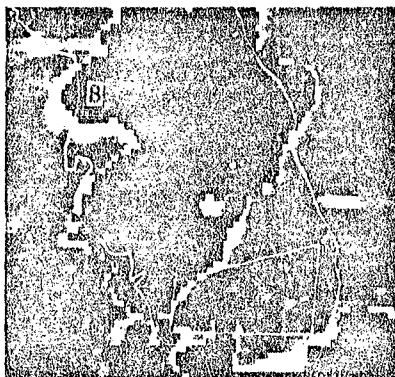
ORIGINAL PAGE IS
OF POOR QUALITY



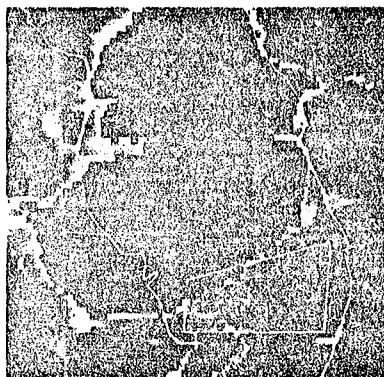
2200 GMT



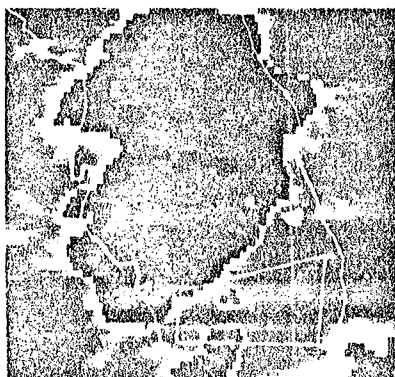
2330 GMT



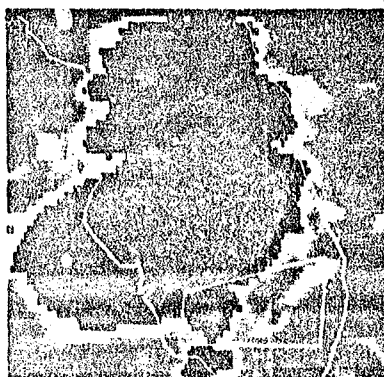
2230 GMT



0000 GMT



2300 GMT



0030 GMT

Figure 6. GOES infrared imagery 2200-0030 GMT 31 July 1980.

ORIGINAL PAGE IS
OF POOR QUALITY

in the GWT so that the dominant parameters in the rain estimation can be identified. Figures 7-13 summarize, for one day and for one limited area, the cloud-derived statistics for the GWT parameters.

a) *Cloud definition*

Figure 7 shows the number of GWT defined clouds as a function of time of day. Total clouds peaked near midday (1800) after which the anvils of convective clouds begin to merge, and the total number of clouds decreases to 3-4 after 2200. At any given time, only about half the clouds are defined as the same entity on the previous image ("old" clouds). Concurrently, very few "new" clouds formed; about half the entities at any time are the result of mergers or splits of previously existing entities.

b) *Cloud lifetime*

Figure 8 summarizes the observations of 53 entities between 1600 and 0100 GMT. 85% had lifetimes of 1 h (two images) or less. Only one entity was observed to exist without interaction through six images. This storm (in Fig. 4, labelled "A") will be discussed at length in a later section.

c) *Cloud area*

The 53 entities provided 95 observation-times of cloud parameters. Figure 9 reveals that while 79% of the sampled clouds were small (less than 5000 km²) a wide variation existed in cloud area. Not all the 95 points can be described as thunderstorms; an examination of the imagery shows that the small entities tend to be cirrus debris, while the largest ones tend to be aggregates of many thunderstorms in various phases of their life cycles.

d) *Fractional area of precipitation*

The inferred echo area term (A_e) in (1) is actually a product of two terms, the maximum cloud area (A_m) and the fractional area of precipitation (A_e/A_m). This empirically derived ratio is shown in Fig. 10. Because the sampled clouds had brief, GWT-defined lifetimes, entities tended to be near

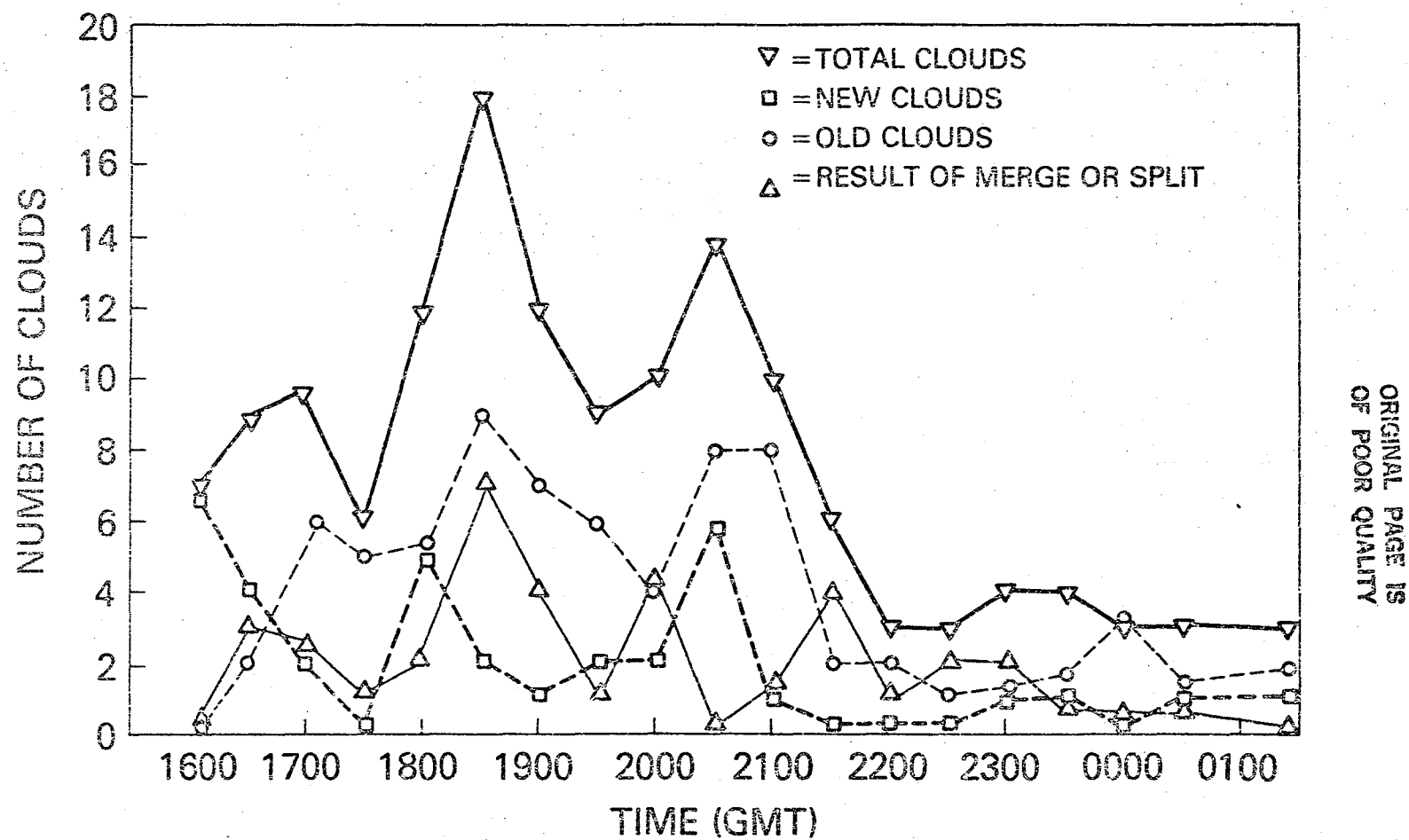
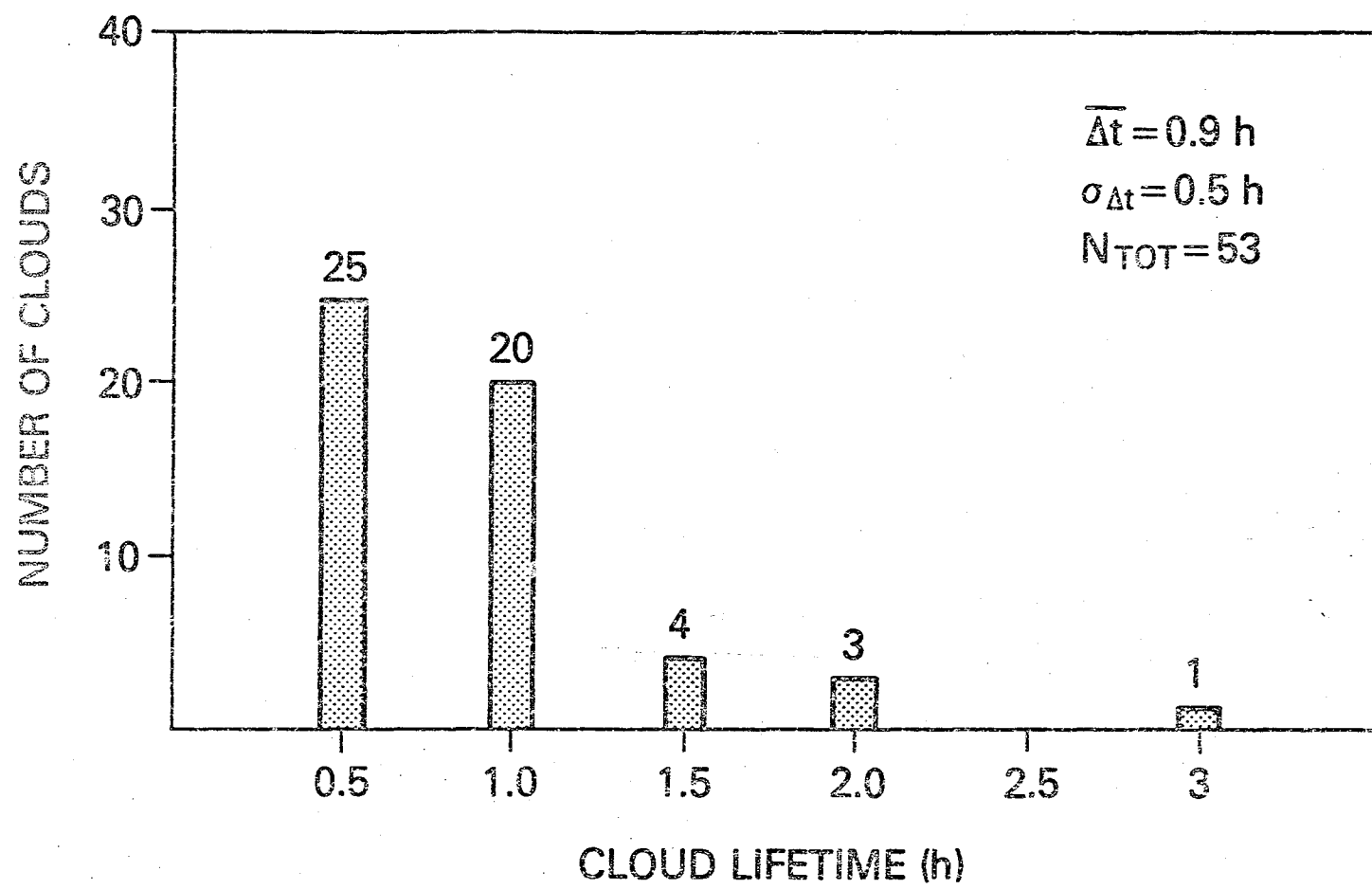


Figure 7. Number of GWT defined clouds as a function of time of day for the data in Figs. 4-6.



ORIGINAL PAGE IS
OF POOR QUALITY

Figure 8. Histogram of cloud lifetime for the 53 entities in Figs. 4-6.

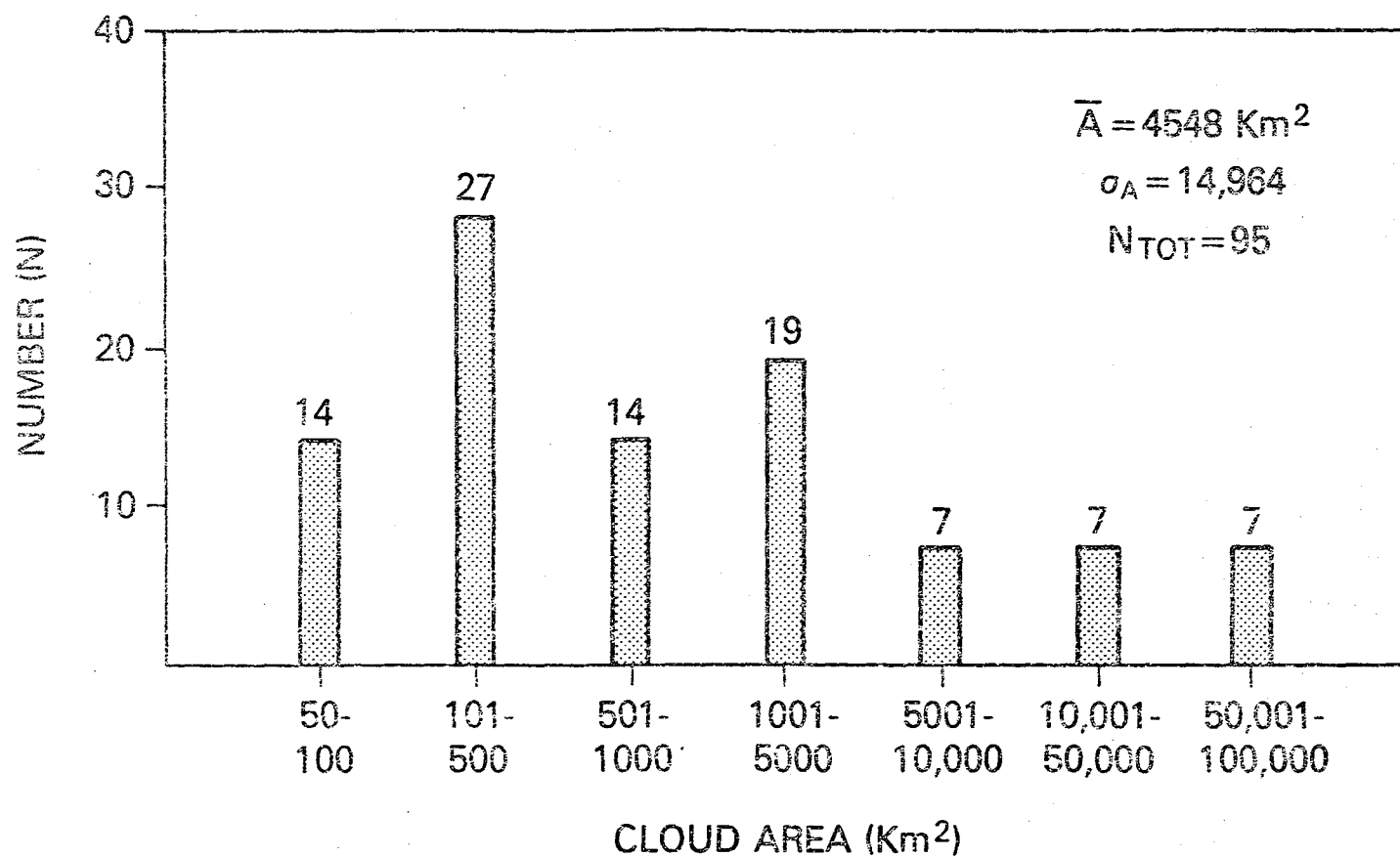
ORIGINAL PAGE IS
OF POOR QUALITY

Figure 9. Histogram of cloud area ($< 253\text{K}$) for the 95 observations of the 53 cloud entities.

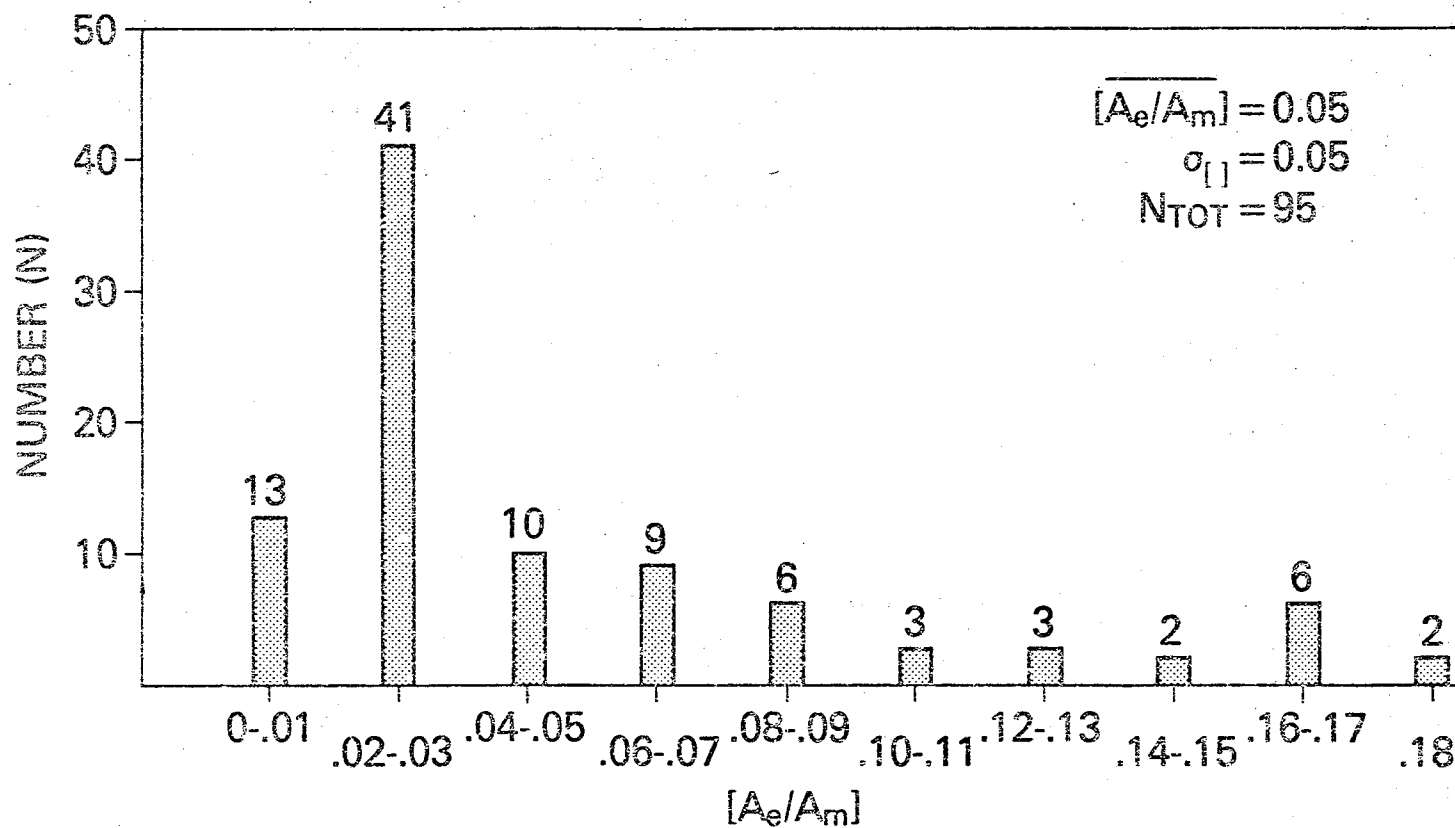
ORIGINAL PAGE IS
OF POOR QUALITY

Figure 10. Histogram of the ratio (echo area/maximum cloud area) for the 95 observations.

or at their maximum area. As a result, the value of 0.02 for A_c/A_m was invoked most often (see Fig. 1 when $A_m < 2000 \text{ km}^2$ and when $A_c/A_m \approx 1$). This value of 0.02 is used for the calculation of R_v and should not be confused with the 50% area of the cloud over which the rain is ultimately apportioned. The ratio A_c/A_m had a mean and standard deviation of 0.05.

e) *Rainrate*

Figure 11 shows the histogram for the nine possible values of rainrate in the GWT (though two are identical). 61% of the data sample had the value (20.7 mm h^{-1}) that occurs when $A_c = A_{c(\text{max})}$ (Fig. 2). The parameter had a small standard deviation with respect to its mean.

f) *Temperature weighting*

Given two clouds of equal area, the summation term in (1) is designed to increase the rain volume for the cloud with the colder internal temperature structure. The distribution of this term is shown in Fig. 12. 55% of the sample had no temperatures below 225K, hence the term was identically 1.0.

g) *Rain volume*

The relationship between GWT computed rain volume and cloud area (Fig. 13) is interesting because A_c does not explicitly appear in (1); it appears indirectly in A_m and in the life history relationships from which the A_c/A_m ratios are derived. Figure 13 is a plot of R_v vs. A_c for the 95 observations. The two are highly correlated ($r = 0.88$) despite the two obvious classes of data. The data were stratified by entities increasing in area (27), decreasing in area (3), entities at their maximum area as part of a life history (43), and entities for which only a single observation existed (22). The GWT empirical relationships for both rainrate and fractional echo area are asymmetric with respect to A_m (refer to Figs. 1 and 2). Hence estimated R_v can be one or two orders of magnitude greater for clouds defined as increasing in area. Very few entities decreased in area; by this stage in their life cycle they tended to split or merge. Some implications of this relationship are discussed in the following section.

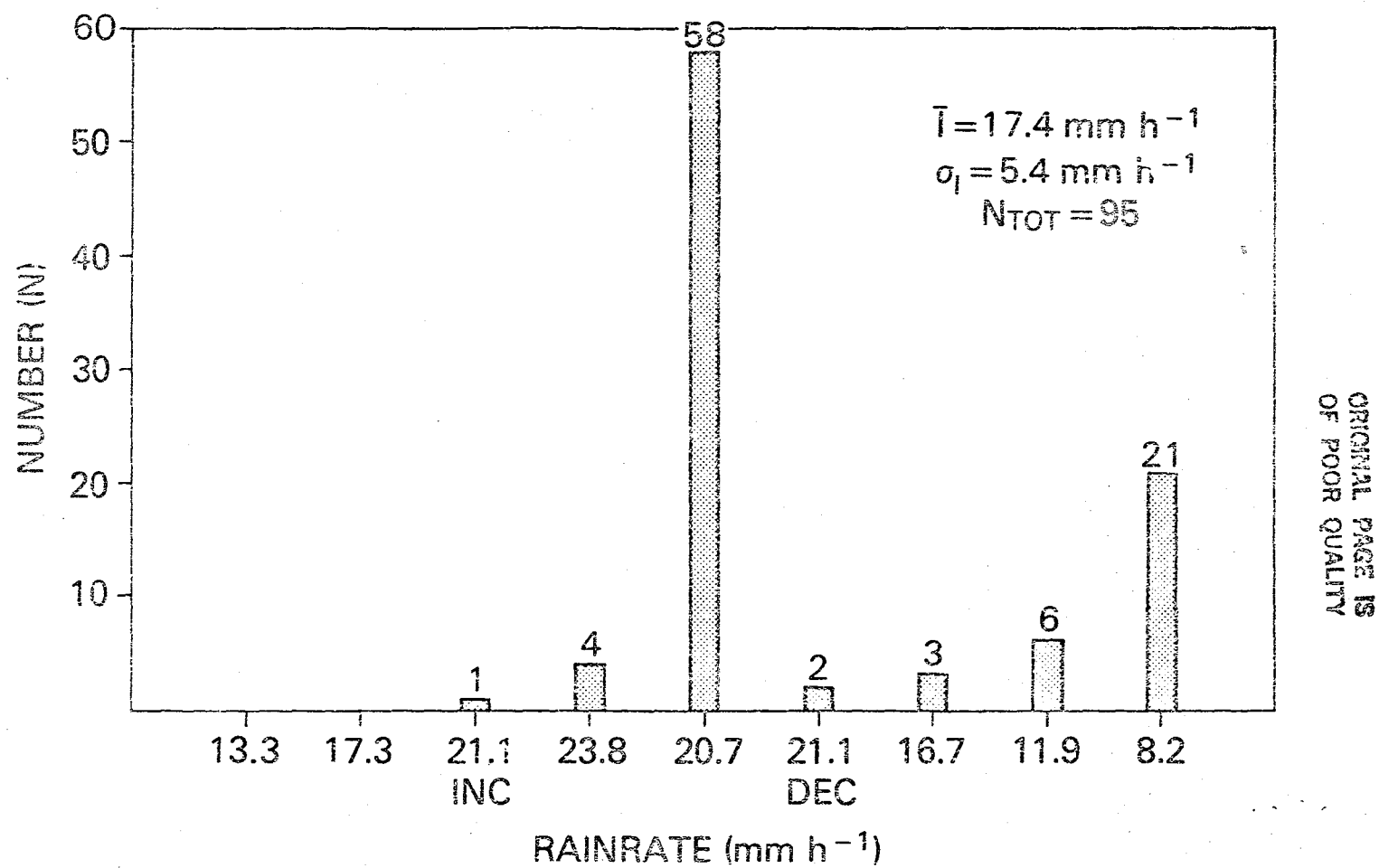
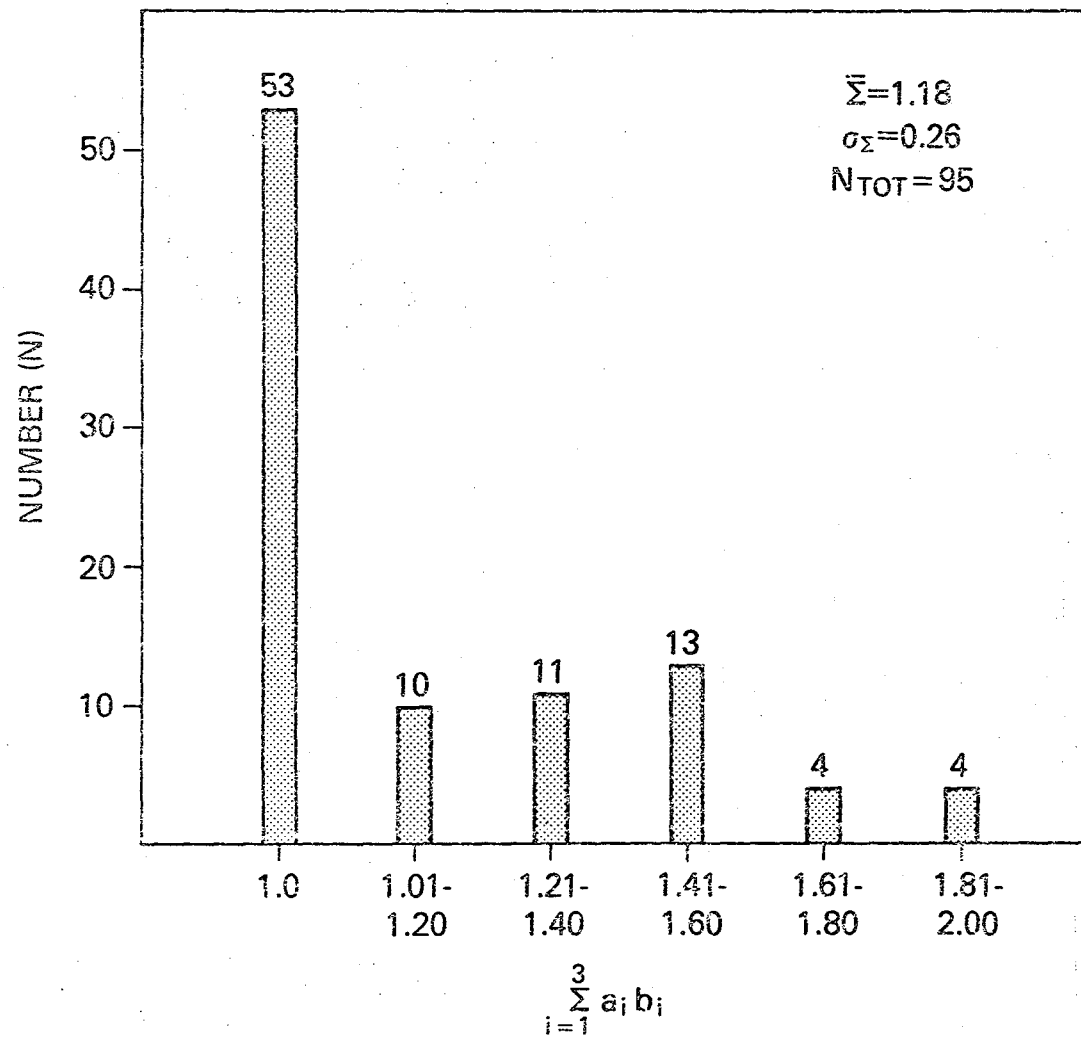
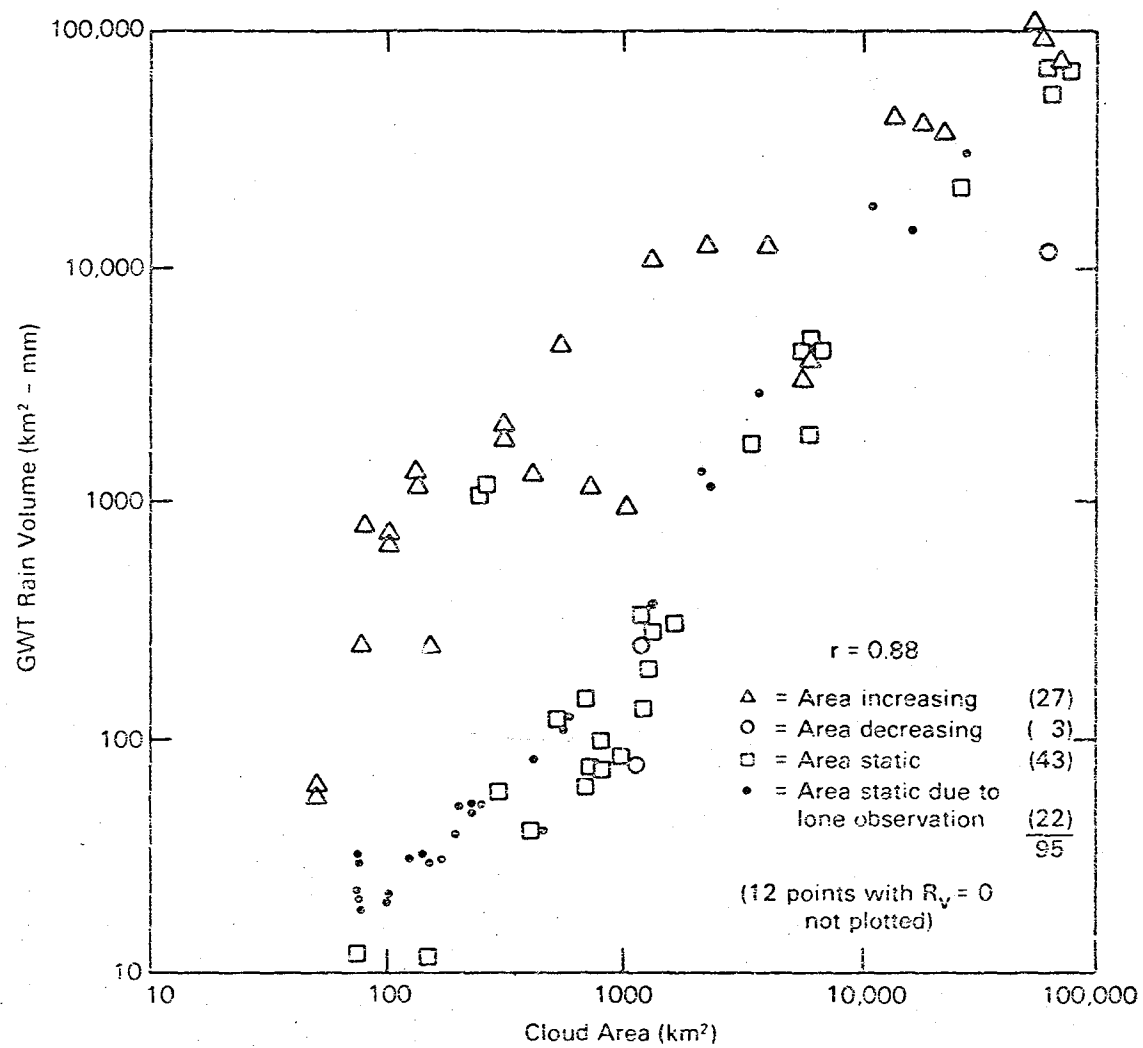


Figure 11. Histogram of the rainrate term for the 95 observations.



ORIGINAL PAGE IS
OF POOR QUALITY

Figure 12. Histogram of the weighting term for the 95 observations. The a_i and b_i are defined in the text.



ORIGINAL PAGE IS
 OF POOR QUALITY

Figure 13. Log-log plot of GWT computed rain volume versus cloud area. Data are stratified by the tendency of area change.

5. DISCUSSION

Though the data presented in Figs. 7-13 are for one day, we believe that the convective development on this day is representative of the Florida area (where the GWT relationships were developed). We believe that the statistics would be similar on any convectively active Florida day. The impression one gains, based on these data, is that the life history approach may not be necessary to produce daily maps of satellite derived precipitation. This is *not* to say that clouds (thunderstorms) do not *have* a life cycle similar to that envisioned by Griffith *et al.* (1976) nor is it to say that these thunderstorm-rain relationships are independent of storm life cycle. Instead we are stating that the conceptual life cycle model proposed by the GWT is not applicable when clouds are defined by the 253K isotherm. It was noted in this limited data sample that the "average" cloud only lasted 1 h before interacting with another. Only 3 of the 95 entities ever decreased in area. Most clouds life histories were terminated prematurely by mergers or splits. In summary, cloud entities defined by the 253K isotherm did not undergo life cycles as depicted by the GWT conceptual model. In fact, Woodley *et al.* (1980) state that few simple, single clouds are ever encountered.

The most long-lived cloud entity was the aforementioned storm west of the FACE target area between 1600 and 1830 (storm "A" in Fig. 4). Its life history (see Fig. 14) consisted of a steady growth over 3 h (dashed curve), terminated by a split. The bracketed numbers above the curve are the values of $\sum_{i=1}^3 a_i b_i$ at each time. Normalizing each A_c by A_m (5862 km²) one can derive the life history of echo area (solid lower curve) and from that, infer rainrate (I). The product of I, A_e , the summation term ($\sum_{i=1}^3 a_i b_i$), and Δt produce the rain volume (top curve). The numbers in parentheses above this curve are the entity's minimum IR temperature. The absolute minimum temperature (T_{min}) achieved by this storm (212K) corresponds to its maximum volume rain (12 661 km²-mm). A similar relationship was found by Negri and Adler (1981) for 15 midwest thunderstorms. For this isolated storm, it seems that the GWT is able to simulate the evolution of thunderstorm rain volume. It is instructive however, to consider what the R_v curve would have been had the cloud been terminated at an earlier stage by a merger. In the worst case, we assumed

ORIGINAL PAGE IS
OF POOR QUALITY

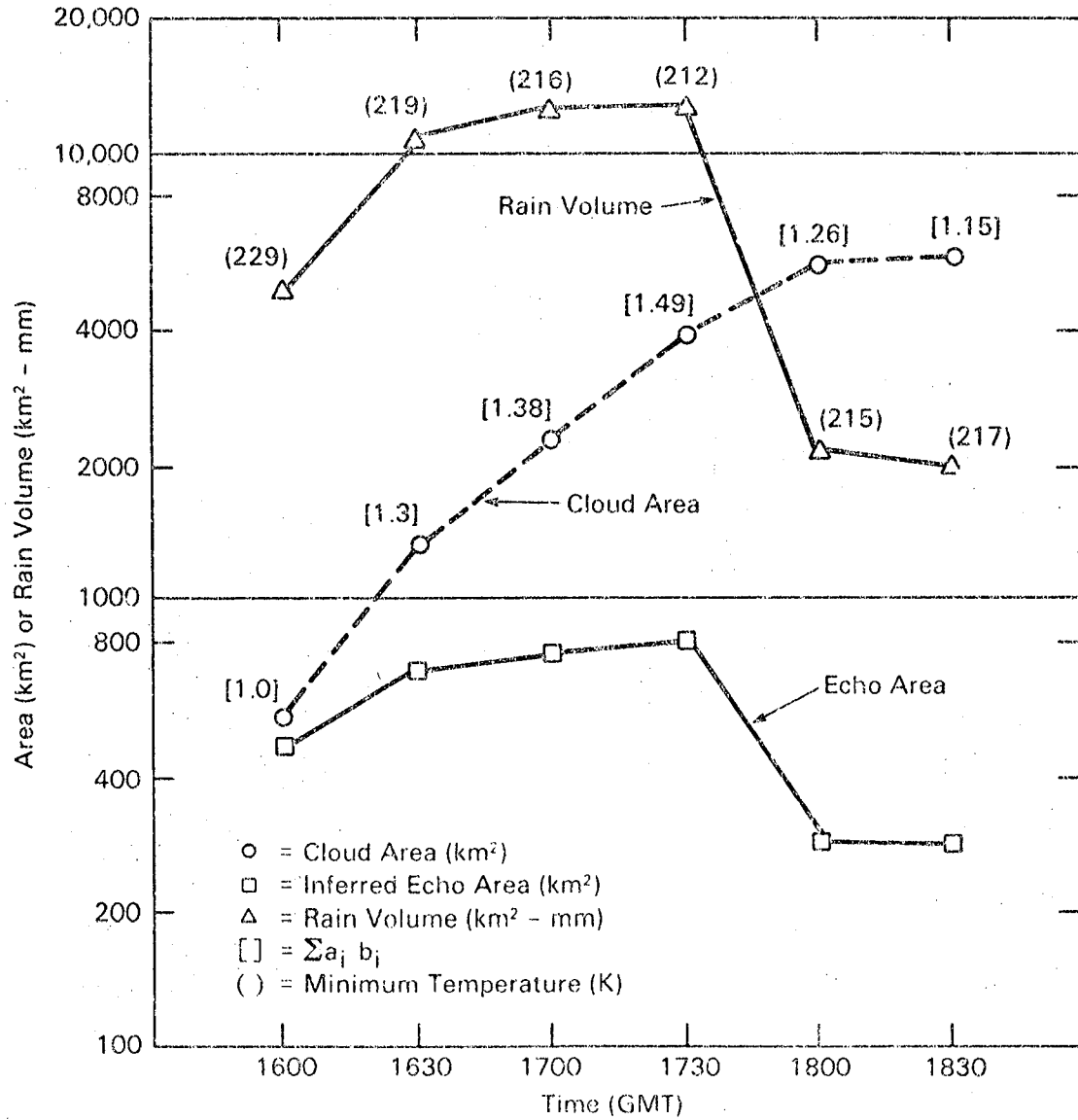


Figure 14. Sample GWT calculation for storm "A", west of the target area in Fig. 4. Cloud area (dashed line) is the primary measurement.

that the cloud existed for only one time step before it merged (at each time step) with a hypothetical cloud whose area was insignificant compared to that of the original storm. Applying the GWT relationships to these individual entities at six different times generated a radically different profile (Fig. 15). The shaded area represents the difference in rain volume solely due to termination criteria. While it is clear that growing clouds produce more rain, in the GWT two clouds of equal size can have two orders of magnitude difference in rain volume depending on whether they happen to grow in clear or cloudy areas. Clouds growing in close proximity to others clouds stand a greater chance of anvil interaction (hence redefinition and less estimated rain) than do identical, isolated clouds. This result appears to be arbitrary and without physical basis. Note also that this cloud does decrease in area (cloud A' in Fig. 5). Its life history has been artificially terminated by a split at 1900 GMT.

Another example of a storm whose life cycle is prematurely terminated by the GWT criteria is the storm labelled "B" beginning at 1800 (Fig. 4). Subjectively, the entity can be followed for over four hours. It can be seen to reach its maximum extent at 2000 after which it decreases in area and disappears (warms) at 2230. In the GWT definition, this storm frequently merges with the anvils of neighboring storms, becoming a small part of the large cloud mass at 2200.

Among the cloud parameters in the GWT, the distributions we calculated for rainrate, fractional echo area, and the temperature weighting term tended to concentrate at one particular value. When combined with the data that suggest that cloud entities are not long-lived, (hence close to their maximum area at any time) it is not surprising that R_v is well related (Fig. 13) to A_c ($A_c = A_m$ for many of the observations). A linear relationship in A_c accounts for 77% of the variance in GWT rain volume. That is, the simple *occurrence* of cloud, more than any other parameter, dominates the calculation of R_v . Simple relationships between cloudiness and rain have been found in several previous studies. Stout *et al.* (1979) showed correlations as high as 0.90 between cloud area and volume rainrate for subjectively defined clouds. Arkin (1979) calculated 6 h averages of

ORIGINAL PAGE IS
OF POOR QUALITY

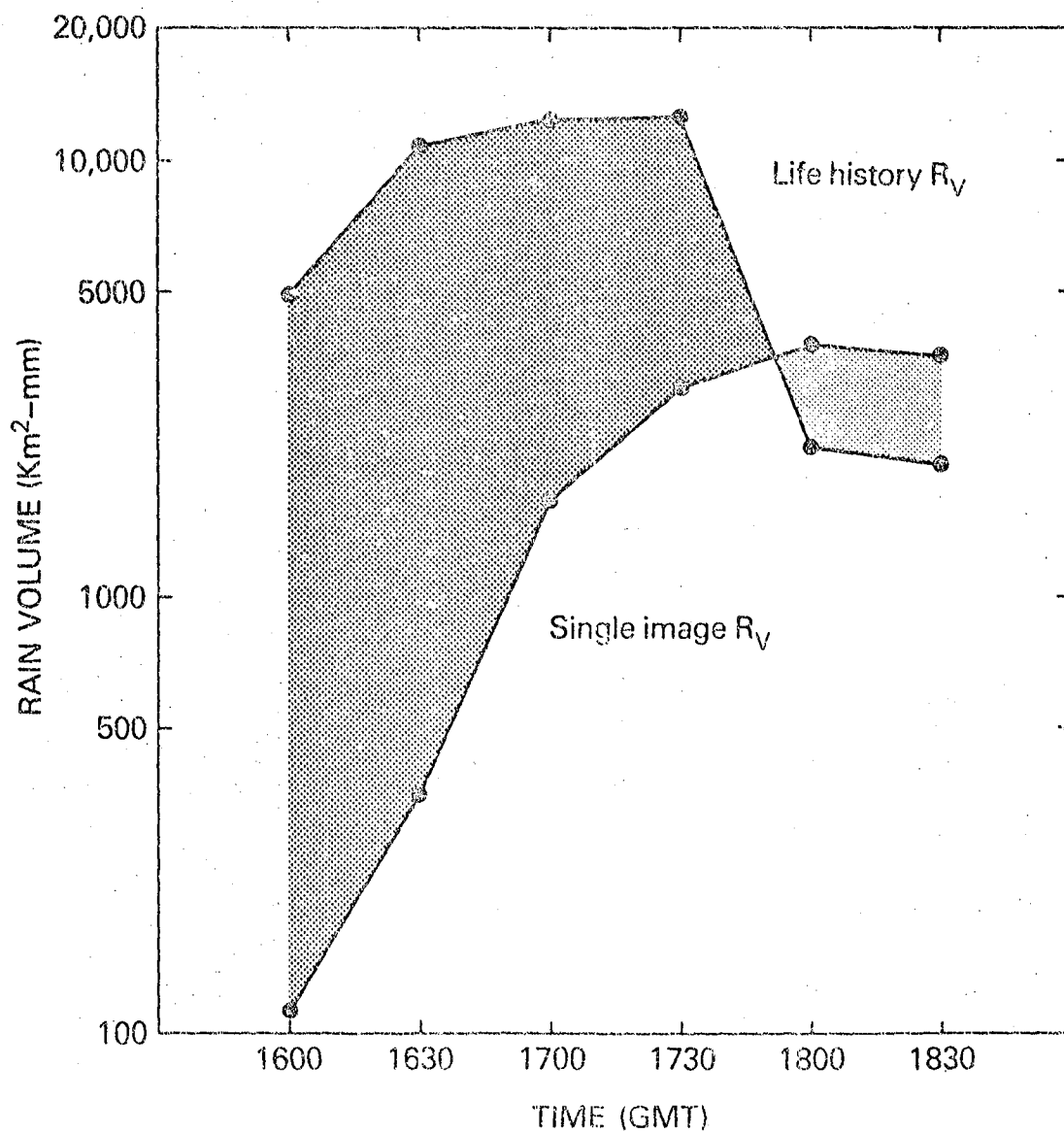


Figure 15. Extreme values of GWT-computed rain volume for the cloud entity of Fig. 14. Stippled regions represent differences in rain volume between the life history computation (top curve) and terminating the entity every 30 min (bottom curve).

ORIGINAL PAGE IS
OF POOR QUALITY

cloud cover colder than 245K and found that to be highly correlated (0.88) with 6 h accumulated rainfall. On monthly time scales, the simple occurrence of cloud is correlated (0.75) with total rain (Kilonsky and Ramage, 1976). Similarly, Lovejoy and Austin (1979) found that GOES IR data are good for determining rain area but poor for determining rain rates. Secondly, Fig. 13 suggests that knowing the tendency of A_c may further refine the rain volume estimate. Stout *et al.* (1979) also noted the lesser importance (a factor of about two) of the area change term.

6. PROPOSED SIMPLIFICATIONS

We consider a cloud with area A_c defined by the 253K isotherm and with temperatures $T_{10\%}$ and $T_{50\%}$ defining its coldest 10% and next warmest 40% areas respectively. Assume also that the cloud has a minimum temperature T_{min} . We may compute from (2a) or (2b) the corresponding values $b_{10\%}$, $b_{50\%}$, and b_{max} . If we assume that the temperature distribution within this area is uniform (all the T_{ij} and hence all the b_{ij} are identical) then

$$(\Sigma b)_{10\%} = .10 N_T b_{ij} \quad (4)$$

where N_T is the number of cloudy (<253K) pixels. Substituting (4) into (3) and noting that $a_{ij} \times N_T$ (area/pixel \times number of pixels) equals A_c , (3) becomes:

$$D_{10\%} = 5R_v/A_c \quad (5a)$$

This states that half the rain volume is distributed *equally* among the pixels (grid squares) of the coldest 10% area. To test this assumption of temperature homogeneity in the 10% area we looked at the "worst" case for each of the 95 entities: at T_{min} the difference ($b_{max} - b_{10\%}$) is maximized. Figure 16 shows this term expressed as a percentage of $b_{10\%}$. For more than half the sample, the point of minimum temperature was the 10% temperature, so that $b_{max} = b_{10\%}$. The mean value was 2.2%, the highest 18%. These are the extreme values; for temperatures warmer than T_{min} the error in the approximation is less.

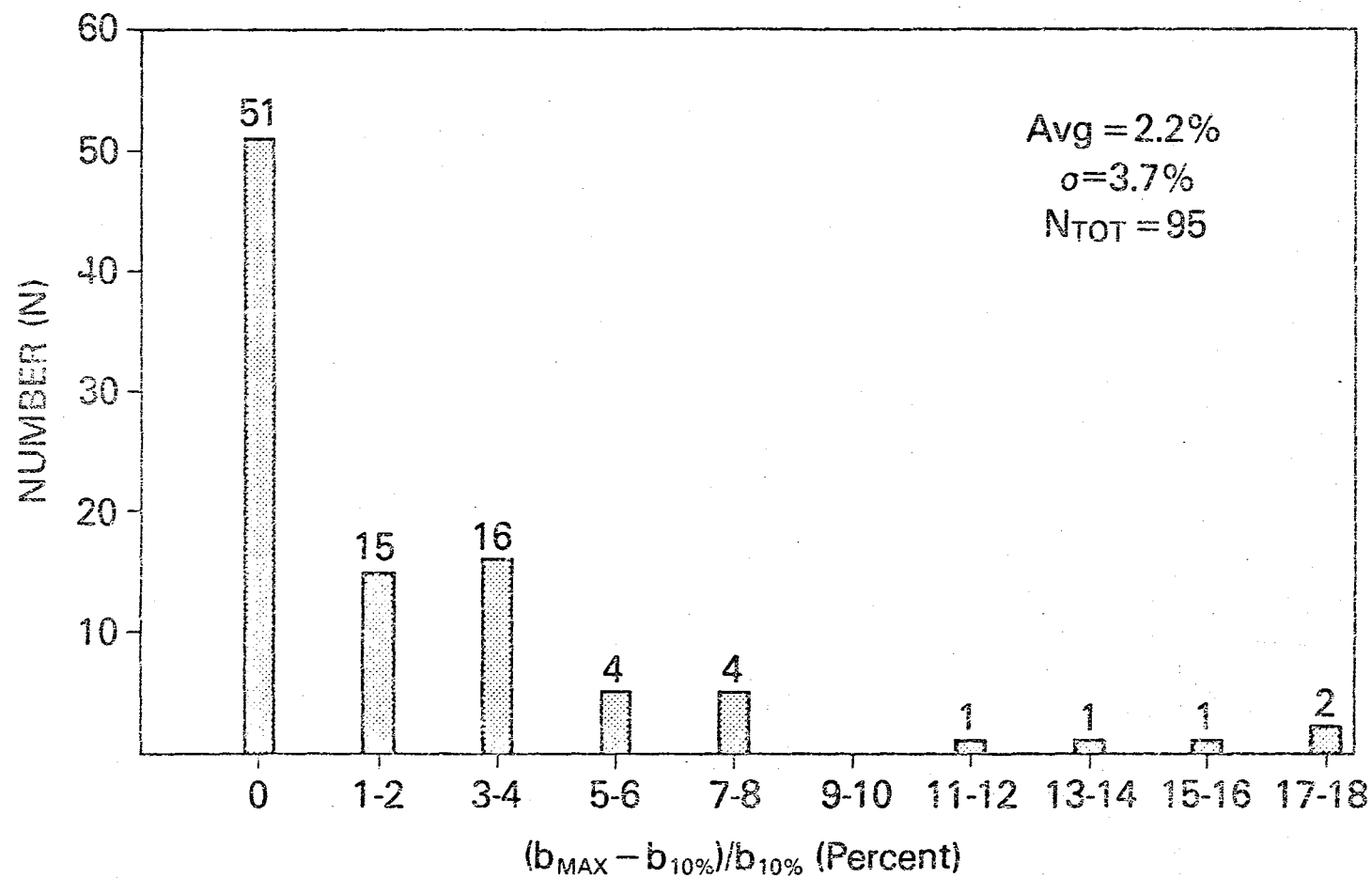


Figure 16. Histogram of the percent error introduced by the assumption that the temperature distribution is uniform within the coldest 10% cloud area.

**ORIGINAL PAGE IS
OF POOR QUALITY**

A similar approach may be applied to the next warmest 40% area:

$$D_{40\%} = 1.25R_v/A_c \quad (5b)$$

The error in the approximation $(\Sigma b)_{40\%} = 0.4N_T b_{ij}$ is shown in Fig. 17. A point with temperature just warmer than $T_{10\%}$ has a value $b_{11\%}$. The "warmest" value is $b_{50\%}$. The error in this approximation is greater: mean 13.6%, extreme 44%. However, this is the worst case. As the temperature of the pixel approaches $T_{50\%}$ the error in the approximation decreases.

Figure 18 shows that the distribution of $T_{10\%}$ for the 95 entities is quite uniform over a wide temperature range. It is here that the GWT's greatest strength appears to be: by apportioning half the rain volume to this area (whether equitably or as a function of pixel temperature) the GWT can produce rain in small (warm) clouds while points at the same temperature in clouds with colder temperatures elsewhere will not produce rain. Figure 19 is the distribution of $T_{50\%}$ and also displays no pronounced peak.

We make one final assumption before applying the simplifications to actual data. The most simple and direct relation between clouds and rain is one where $R_v \propto A_c$, and is substantiated by the correlation of Fig. 13 and by correlations found by others. In the simplest case, $R_v = k \times A_c$. We have subjectively let $k = 1 \text{ mm}$, the calculated slope of a regression line fit to Fig. 13. Then (5a) and (5b) become:

$$D_{ij} = 5 \text{ mm} \quad (T_{ij} < T_{10\%}) \quad (6a)$$

$$D_{ij} = 1.25 \text{ mm} \quad (T_{10\%} < T_{ij} < T_{50\%}) \quad (6b)$$

These equations are independent of cloud life history, independent of cloud area, and independent of grid square area.

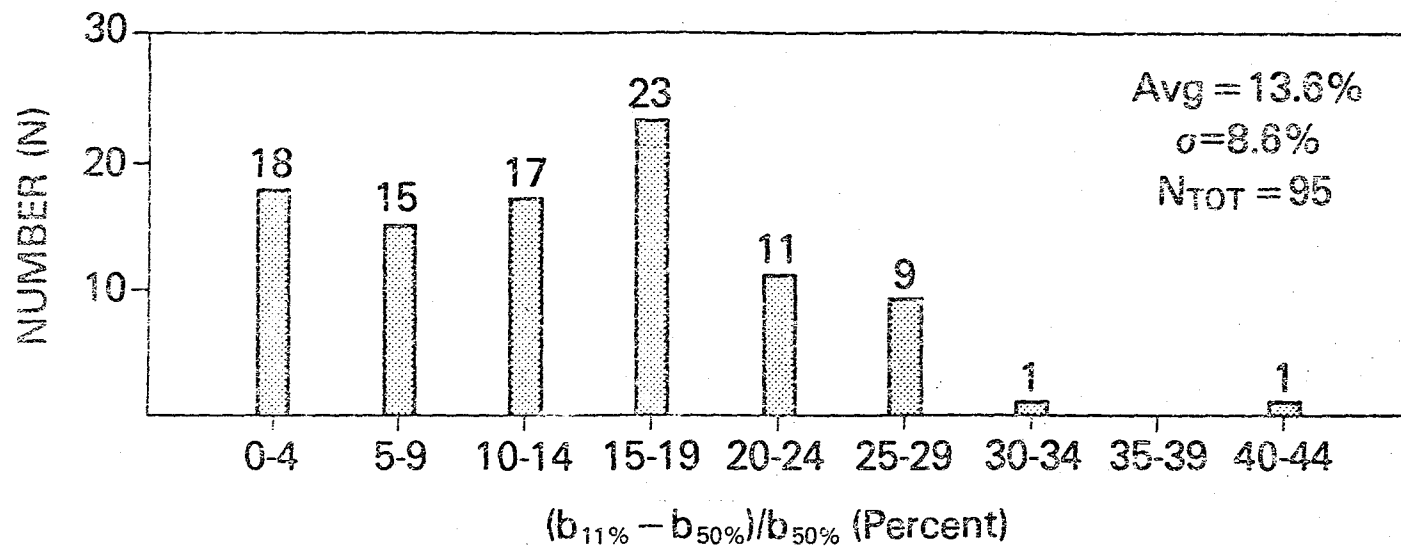
ORIGINAL PAGE IS
OF POOR QUALITY

Figure 17. Histogram of the percent error introduced by the assumption that the temperature distribution is uniform within the next warmest 40% cloud area.



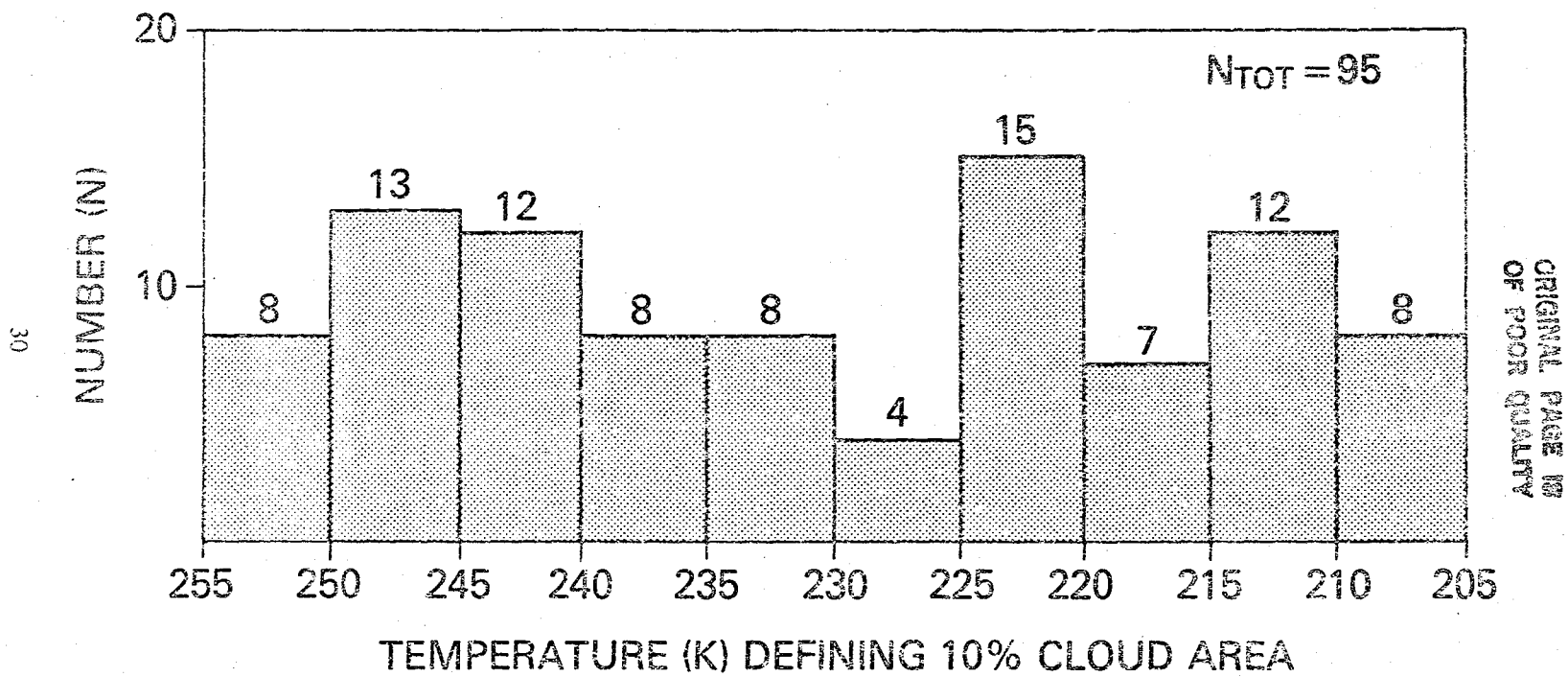


Figure 18. Temperature (K) that defines the coldest 10% cloud area.

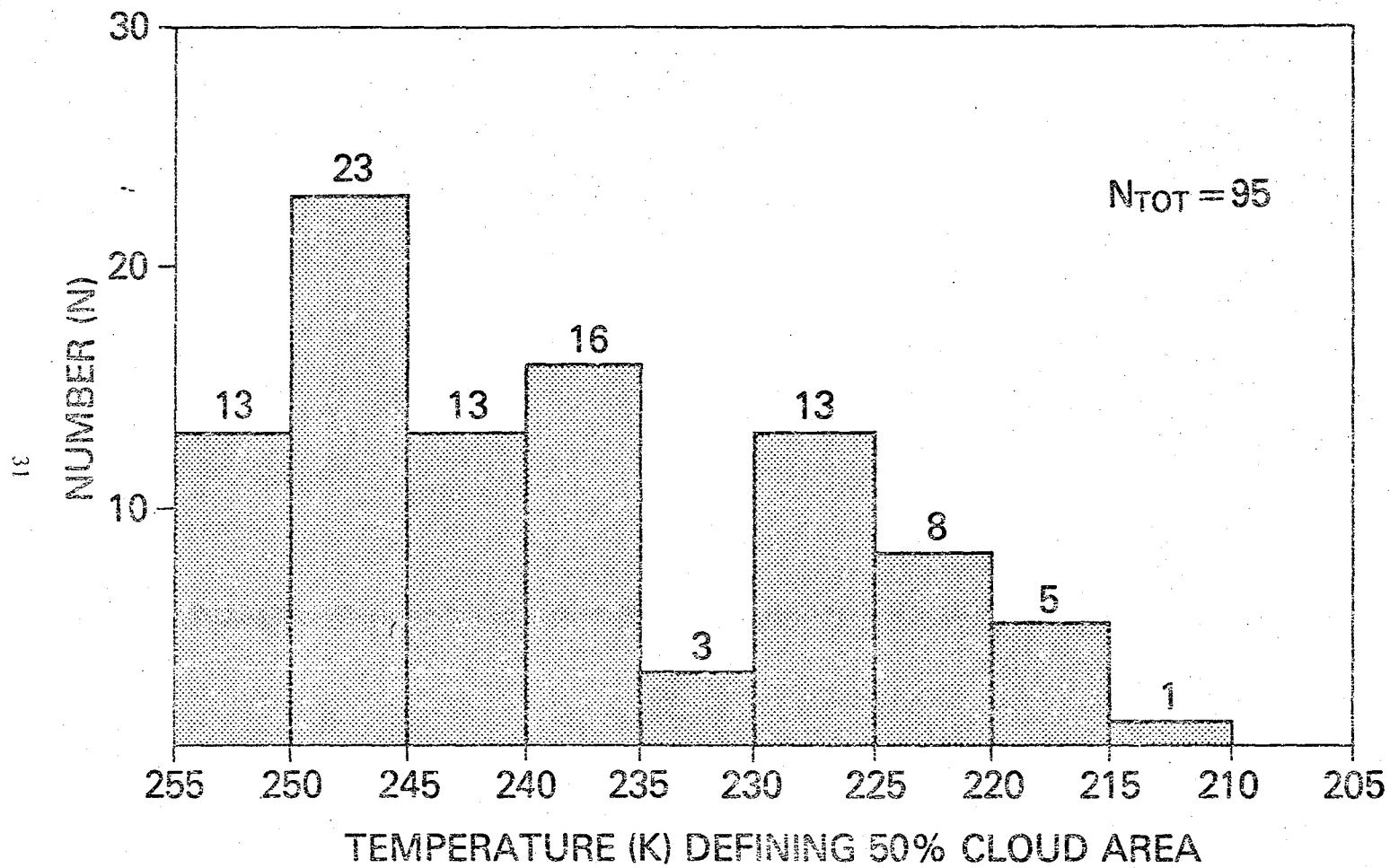


Figure 19. Temperature (K) that defines the next warmest 40% cloud area.

ORIGINAL PAGE IS
OF POOR QUALITY

7. RESULTS

Implicit in equations (6a) and (6b) are the variables $T_{10\%}$ and $T_{50\%}$, the temperatures that define the coldest 10% and 50% of the cloud entity. Because we choose not to define individual clouds, we looked at histograms of CTT for the 500 by 500 km region of Figs. 4-6. The variation of the threshold temperatures as a function of time of day is shown in Fig. 20. They undergo a diurnal variation of as much as 25K. We then applied these thresholds to the FACE extended area, a region 8° of latitude by 12° of longitude. In this case, the (ij) grid squares represented an area of about 13 km^2 . On the AOIPS, equations (6a) and (6b) were implemented using a lookup table that converts counts (temperature) to rain depth. For example, on the 1600 GMT image, pixels warmer than 233K receive no rain, pixels between 232 and 223K each receive 1.25 mm and pixels colder than 223K receive 5 mm. Each satellite IR image, with the lookup table applied, represents a half-hourly rain estimate map which can be summed for any time period.

The result (Fig. 21) is an isohyetal map of satellite derived daily rainfall in GOES coordinates, with gray shades representing rain depth (mm). This should be compared to Fig. 22, the isohyets derived from the time dependent GWT (reproduced from Meitin *et al.*, 1981). Because clouds (in particular cold clouds) are highly correlated with rainfall, it is not surprising that the schemes produce similar results. It should be remembered that neither method represents ground truth, but rather estimates based on satellite nephanalysis. The two maps agree well for the large, circular rain area off the southeast Florida coast, for the three-celled maxima in the southwest quadrant, and for the lighter rain regions off the east coast of Florida. The only notable difference is that the GWT 40 mm maximum due west of the target area is underestimated in the simplified method. This was caused by the long lived, isolated thunderstorm discussed previously. It is not possible to say which display is representative of the true rainfall for one particular storm. A comparison is possible for the FACE target area. Daily (1630-0100 GMT) rain volumes for this area were 2.84, 2.34, and $2.68 \times 10^7 \text{ m}^3$ using the GWT, gages, and the simplified equations, respectively. This was a day of relatively small rainfall in the FACE area. This comparison indicates that daily rain

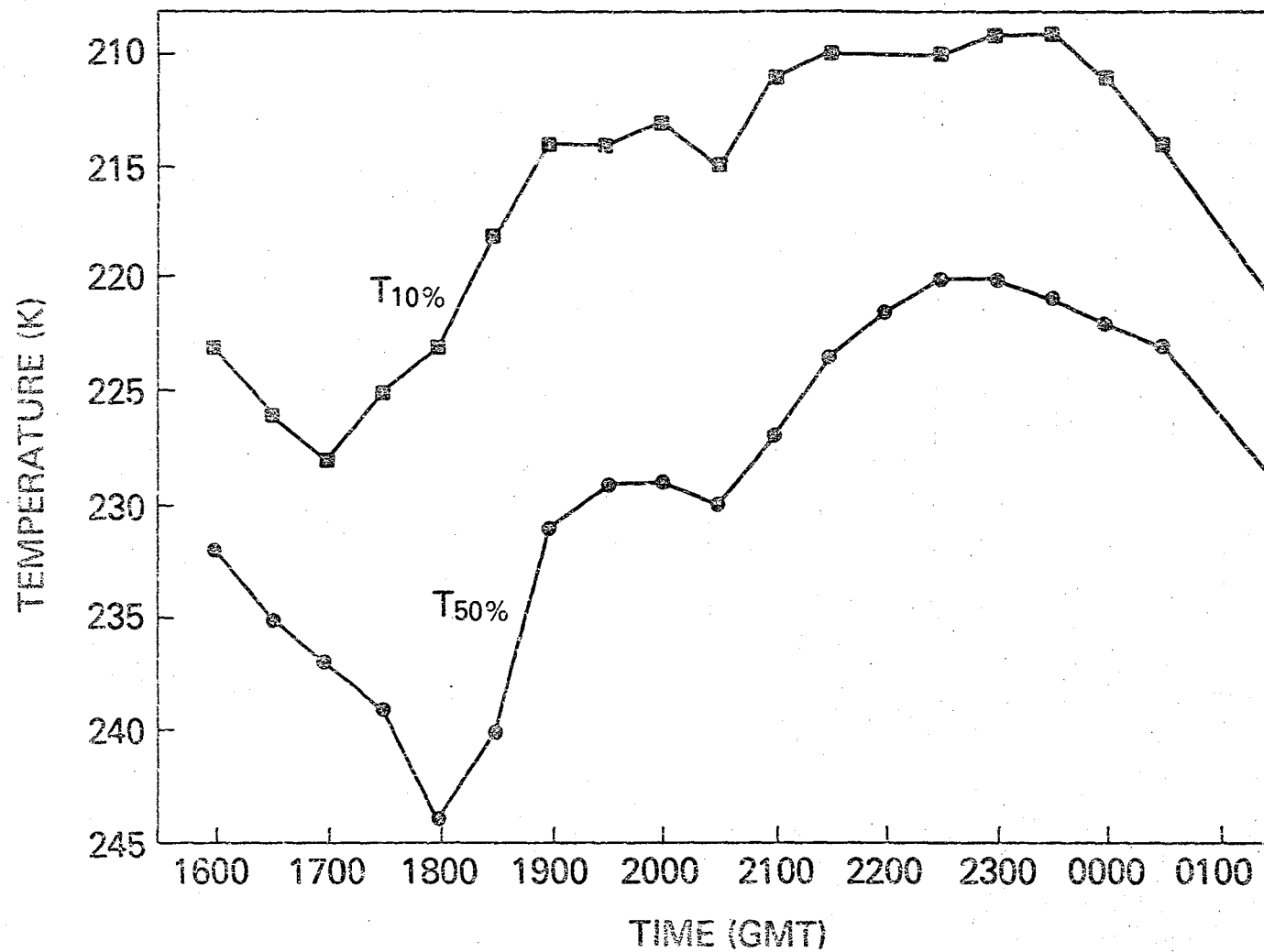
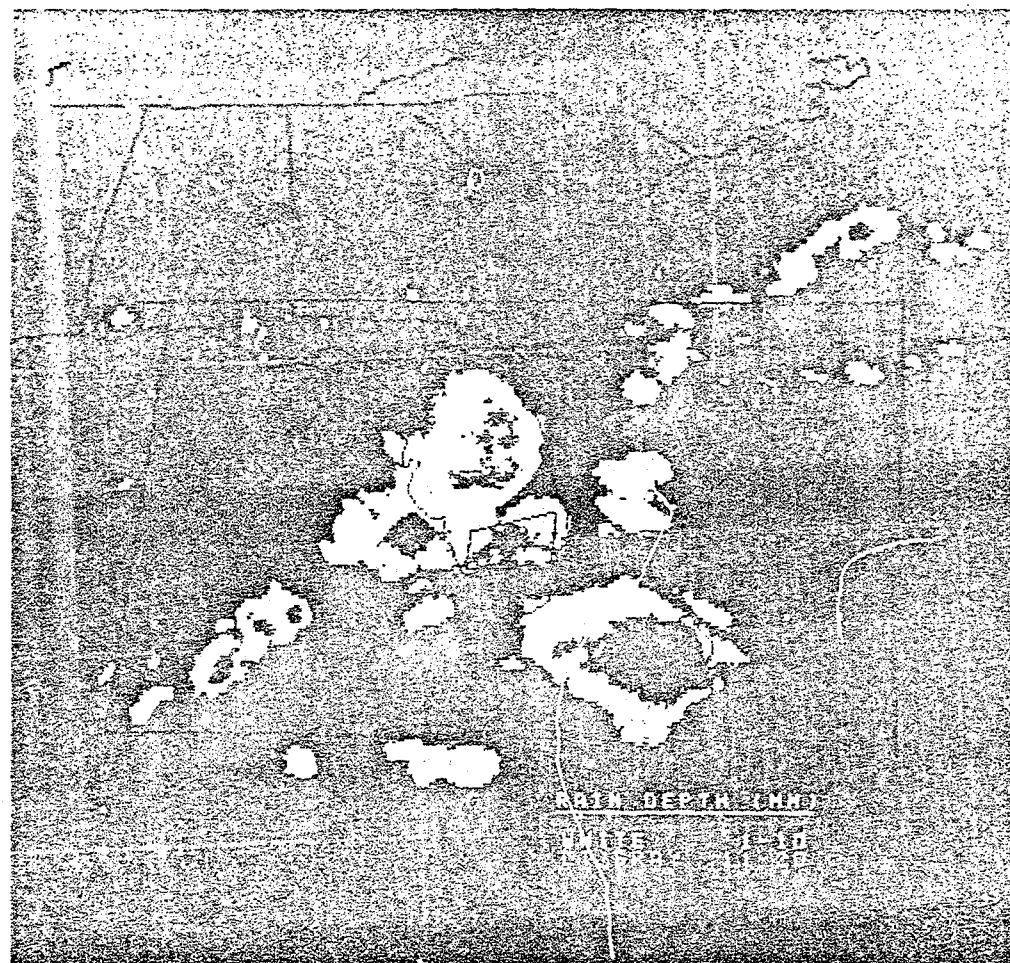


Figure 20. The temperature thresholds as a function of time of day for *total* cloudiness in the regions shown in Figs. 4-6.

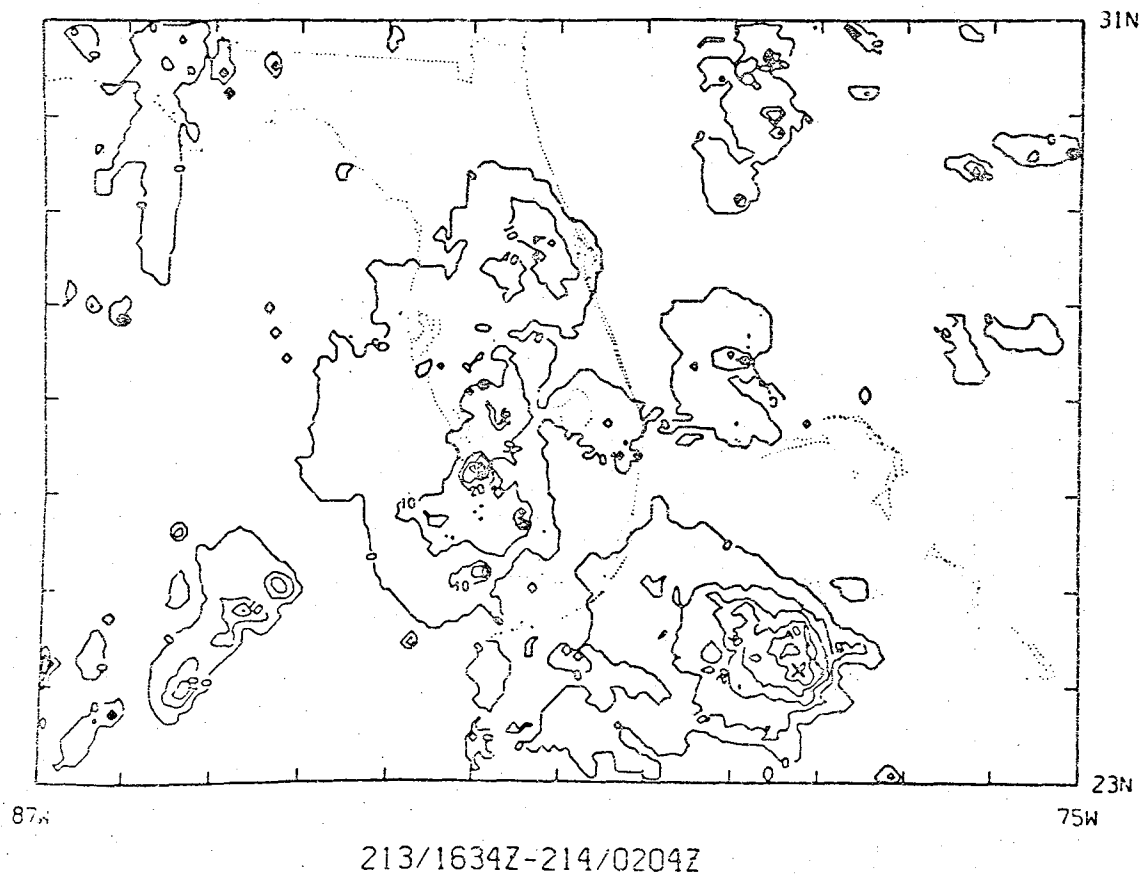
ORIGINAL PAGE IS
OF POOR QUALITY



ORIGINAL PAGE 19
OF POOR QUALITY

Figure 21. Satellite derived rainfall (mm) for the FACE extended area (large trapezoid) for the period 1600-0130 GMT, the result of applying equations (6a) and (6b) to a sequence of IR imagery. The coordinate system is that of the eastern GOES, and the gray scale is shown.

FACE SATELLITE RAINFALL
31 JULY 80
UNADJUSTED



ORIGINAL PAGE IS
OF POOR QUALITY

Figure 22. GWT derived rainfall for the period 1630-0200 GMT. Contours are every 10 mm beginning at zero. (From Meitin *et al.*, 1981).

ORIGINAL PAGE IS
OF POOR QUALITY

estimates comparable to those of the GWT can be made from a more straightforward technique. Further testing on additional days should confirm this finding.

8. CONCLUSIONS

It was not the objective of this study, nor was it possible, to evaluate the GWT by lengthy statistical analyses of many data sets. Rather for one day and for one limited area, the magnitude and variability of the terms in the GWT equations were explored. The day was typical of convective development over Florida, where the GWT was developed. The concept of life history was examined via specific examples of satellite imagery (heretofore unrepresented in the GWT literature).

Due to the definition of cloud entities by an anvil edge temperature (253K), a simple model of cloud growth and decay (Griffith *et al.*, 1978) did not exist for most of the GWT-defined entities. Only about half the entities were defined on two successive images; about half the entities at any time were the result of mergers or splits. Because such entities were close to, or at, their defined maximum area for most of their lifetime, the empirically derived ratio A_e/A_m was the singular value 0.02 for 43% of the data sample. Similarly the derived quantity A_e (echo area) typically had little life history, forcing the rainrate term (I) to be 20.7 mm h^{-1} for 61% of the sample. The summation term was identically 1.0 for 55% of the sampled clouds.

One parameter with wide variability is the cloud area (A_c). While this parameter does not explicitly appear in the GWT equations, it is highly correlated (0.88) with computed rain volume. Clouds increasing in area have up to 50 times more GWT rain volume than identical static clouds. This effect was more pronounced in small ($< 5000 \text{ km}^2$) clouds. While the concept that growing clouds produce more rain is physically realistic, the GWT has a definite bias towards growing, *isolated* clouds. Such clouds do not interact with other clouds, (hence being artificially redefined) unlike clouds growing in proximity to others. These latter clouds are often defined as having no growth because of continual redefinition.

Any objective scheme for defining clouds will have shortcomings. However, interactions between entities defined at 253K often involve cirrus anvil debris rather than active convection. Clouds defined by 253K may often represent entities larger than individual thunderstorms. Such entities may be composed of many thunderstorms in various stages of their life cycles. This leads us to conclude that the GWT life cycle conceptual model is not generally applicable to clouds defined by the 253K isotherm, and that the GWT apportionment scheme is unnecessarily complicated for daily rain estimation over large (10^5 - 10^6 km²) areas. On smaller time scales (1-3 h), where a life history approach to thunderstorm rainfall would appear to be realistic, the technique is severely limited by the 0.5-1.0 h average lifetime of a GWT-defined entity.

An important, discriminating parameter in the GWT was found to be the temperature that defines the coldest 10% cloud area. (Note that this is not dependent on cloud life history). However, it was found that within these areas the temperature structure is fairly uniform. This threshold (and a similar one for the next warmest 40% area) decreased by 20K as the convection developed over the Florida area. A simplified algorithm was derived from the GWT equations by assuming:

- 1) The rain volume is a linear function of cloud area at any time;
- 2) The temperature distribution in both the 10% and 40% areas were uniform;
- 3) The temperature thresholds varied with time of day and could be applied regionally rather than to individual clouds.

The resultant equations are independent of cloud life history, cloud area, and grid square area. They are dependent on the grid square being in one of two temperature regimes. By applying the equations to the IR data we derived an isohyetal map very similar to that derived by the GWT. A comparison of daily rain volumes for the FACE target area yielded estimates of 2.84, 2.34, and

$2.68 \times 10^7 \text{ m}^3$ using the GWT, gages, and the simplified equations respectively. It is concluded that the two important parameters in rainfall estimation from satellite IR data are the existence of cold cloud and the duration of cloud over a point.

REFERENCES

- Arkin, P.A., 1979: The relationship between fractional coverage of high cloud and rainfall accumulations during GATE over the B-scale array. *Mon. Wea. Rev.*, **107**, 1382-1387.
- Augustine, J.A., C.G. Griffith, W.L. Woodley and J.G. Meitin, 1980: Insights into errors of SMS-inferred GATE convective rainfall. *J. Appl. Meteor.*, **20**, 509-520.
- Garcia, O., 1981: A comparison of two satellite rainfall estimation schemes for GATE. *J. Appl. Meteor.*, **20**, 430-438.
- Griffith, C.G., J.A. Augustine, and W.L. Woodley, 1981: Satellite rain estimation in the U.S. High Plains. *J. Appl. Meteor.*, **20**, 53-66.
- _____, W.L. Woodley, and J.A. Augustine, 1980: Final report to the Water and Power Resources Service on the estimation of convective, summertime rainfall in the U.S. High Plains from thermal infrared geostationary satellite data, Vol. 1. NOAA/ERL, Boulder, CO.
- _____, _____, S. Browner, J. Teixeira, M. Maier, D.W. Martin, J. Stout and D.N. Sikdar, 1976: Rainfall estimation from geosynchronous satellite imagery during daylight hours. NOAA Tech. Rep. ERL 356-WMPO 7, Boulder, CO, 106pp.
- _____, _____, P.G. Grube, D.W. Martin, J. Stout and D.N. Sikdar, 1978: Rain estimation from geosynchronous satellite imagery: Visible and infrared studies. *Mon. Wea. Rev.*, **106**, 1153-1171.
- Kilonsky, B.J. and C.S. Ramage, 1976: A technique for estimating tropical open-ocean rainfall from satellite observations. *J. Appl. Meteor.*, **15**, 972-975.
- Lovejoy, S. and G.L. Austin, 1979: The sources of error in rain amount estimating schemes from GOES visible and IR satellite data. *Mon. Wea. Rev.*, **107**, 1048-1054.

- Meitin, J.G., W.L. Woodley and C.G. Griffith, 1981: FACE-2 data reductions and analyses: Part V. Satellite estimated rainfall from a geostationary platform in FACE-2. NOAA Tech. Memo. ERL OWRM-11, Boulder, CO, 141pp.
- National Aeronautics and Space Administration, 1981: Workshop on precipitation measurements from space. NASA/Goddard Space Flight Center, Greenbelt, MD, 385pp.
- Negri, A.J. and R.F. Adler, 1981: Relation of satellite based thunderstorm intensity to radar estimated rainfall. *J. Appl. Meteor.*, 20, 288-300.
- Simpson, J. and V. Wiggert, 1969: Models of precipitating cumulus towers. *Mon. Wea. Rev.*, 97, 471-489.
- Stout, J.E. D.W. Martin, and D.N. Sikdar, 1979: Estimating GATE rainfall with geosynchronous satellite images. *Mon. Wea. Rev.*, 107, 585-598.
- Woodley, W.L., C.G. Griffith, J.S. Griffin and S.C. Stromatt, 1980: The inference of GATE convective rainfall from SMS-1 imagery. *J. Appl. Meteor.*, 19, 388-408.

END

DATE

FILMED

FEB 14 1984

LANGLEY RESEARCH CENTER



3 1176 00512 3956